TM No. 941021

NAVAL UNDERSEA WARFARE CENTER - DETACHMENT NEW LONDON

NEW LONDON, CONNECTICUT 06320

Technical Memorandum

A Maximum Likelihood Based Adaptive Detector

Date: 15 April 1994

Prepared By: Douglas A. Abraham

Douglas A. Abraham
Advanced Engineering Division
Submarine Sonar Department

ABSTRACT

Adaptive, frequency domain, array signal detection is considered when there exist data blocks containing interference alone and signal plus interference that are disjoint in time and span several frequencies. The data block solely containing interference is used to form estimates of the interference covariance structure at each frequency. These estimates are substituted into generalized likelihood ratios to form constant false alarm rate detectors for deterministic and Gaussian signals that are limited in time to the signal plus interference data block. Central limit theorem based normal approximations are used to determine thresholds and the signal-to-interference ratio (*SIR*) required to achieve specified false alarm and detection probabilities. The *SIR* required for the proposed detectors is shown to be the *SIR* required for the ideal conventional detector with interference covariance estimation losses and intra-block correlation losses. The gain in adaptive processing (i.e., the reduction in signal strength required to achieve specified false alarm and detection probabilities) is seen to be the ratio of the array gain improvement (*AGI*) to the change in the estimation and correlation losses resulting from the shift from conventional beamforming (dimension equals one) to higher dimension processing. Thus, the *AGI* must exceed the change in the estimation and correlation losses before adaptive detection becomes attractive.

ADMINISTRATIVE INFORMATION

This work was sponsored by the Office of Naval Research.

The author of this memorandum is located at the Naval Undersea Warfare Center, New London Detachment, New London, CT 06320.

The technical reviewers for this memorandum were J. A. Nuttall (Code 2121) and T. E. Luginbuhl (Code 2121).

The author thanks Stephen Greineder, Tod Luginbuhl, and James Nuttall for their careful review. Their comments have considerably improved the quality and presentation of this memorandum.

TABLE OF CONTENTS

Section Page

1 INTRODUCTION 1

2 ARRAY SIGNAL DETECTION BACKGROUND 2
2.1 Pre-Detector Signal Processing 3
2.2 Statistical Modeling 5

3 MAXIMUM LIKELIHOOD BASED ADAPTIVE DETECTORS 7
3.1 Array Data Structure 7
3.2 Detector Derivation 9
3.3 Statistical Description of the Adaptive Beam Output 12

4 DETECTOR ANALYSIS 16
4.1 Signal Time-Frequency Model 16
4.2 Test Statistic Mean and Variance 17
4.3 Detection Performance via CLT 20

5 DETECTOR PERFORMANCE 24
5.1 SIR Decomposition 24
5.2 Typical AGI 26

6 CONCLUSIONS 32

APPENDIX A - PDF OF CFAR AND SIR LOSS RANDOM VARIABLES 35

APPENDIX B - MONTE-CARLO INTEGRATION 39

REFERENCES 40

A MAXIMUM LIKELIHOOD BASED ADAPTIVE DETECTOR

1 INTRODUCTION

Adaptive detection of signals received by an array of sensors provides improved performance over contemporary methods involving conventional beamforming prior to a detection algorithm in interference environments that yield high array gain improvement (*AGI*). Several issues plague adaptive detection, the foremost involves the estimation of unknown covariance matrices. Imperfect knowledge of covariance matrices both degrades performance and complicates the detector derivation and analysis. Detectors are often based on *optimal* techniques drawn from the Neyman-Pearson theory of hypothesis testing. Optimal in this case implies maximizing the probability of detecting a signal given a fixed probability of false alarm. When a complete statistical description of the signal and interference is available, these techniques provide the best detector structure in the form of a likelihood ratio test (LRT). When only partial information about the statistics is available, optimal tests rarely exist and the suboptimal, although usually very good, generalized likelihood ratio tests (GLRT's) are used. Ideally, a detector incorporates known signal information such as time and frequency characteristics into the design of the algorithm. This *matching* of the detector structure to the signal unfortunately means that a loss is incurred if the signal does not have the assumed structure, perhaps due to time or frequency spreading of a transmitted signal, propagation effects of the medium, or simply a lack of knowledge of signal characteristics. A detector that is robust against not only signal mismatch, but also against the general time-frequency characteristics of the signal, is desired.

It is commonly assumed that the interference hindering detection is stationary over a length of time greater than that of the signal. In frequency domain array processing (i.e., discrete Fourier transform (DFT) of the array time data), the signal may be assumed to lie in a block of data in time (consecutive DFT outputs, also called time snapshots) and frequency, denoted the primary data block (PDB). Under the above stationarity assumption, the interferences present in the PDB are also present in data in adjacent, disjoint time snapshots at the same frequencies. This data is grouped and denoted the secondary data block (SDB). The primary-secondary data block structure is shifted in time, continually testing for the presence of a signal in the PDB subject to normalization by the interferences present in both data blocks. Wolcin [1], with extensions by Nuttall [2], has considered such a PDB with exponential averaging of the interference covariance structure over a semi-infinite SDB consisting of all data previous to the PDB. Specific subsets of these general block assumptions are found in the cardinal work of Reed, Mallett and Brennan [3], as well as more recently in several papers, notably by Kelly [4], Robey et al. [5], Robey [6], and Chen and Reed [7]. These papers [3-7] consider the single frequency case where the PDB consists of a single array vector and the SDB is a set of vectors with the same interference covariance

structure. Robey [6] does consider the case of a multiple vector PDB, however, the detector analysis is for the single vector case. These papers are also based on a signal with deterministic form and an unknown complex amplitude.

This memorandum provides a brief background on array signal detection, proposing the use of matrix preprocessing to reduce the adaptive dimension of the detector and discussing common statistical models of the array data. Detectors will be developed and analyzed for the deterministic signals considered in the above references [3-7] as well as a Gaussian signal with unknown power. The detector development is based on a generalization to the likelihood ratio approach reported by Robey [5, 6]. Following Wolcin [1], the detector for the Gaussian signal is designed to account for varying signal time-frequency characteristics by only considering time-frequency cells in the PDB that may contain a signal exceeding a particular strength. This effectively estimates the location of the signal in the PDB time-frequency cells.

The detector performance is evaluated by the signal-to-interference ratio (*SIR*) required to achieve desired false alarm and detection probabilities. When there are enough cells in the PDB, analysis may be performed by a normal random variable approximation using the central limit theorem (CLT). The *SIR* is decomposed into the required *SIR* for the ideal non-adaptive detector (i.e., conventional beamforming prior to detection when the conventional beam output power is known) as reported by Wolcin [1] or Nuttall [2], with losses due to the estimation of the interference statistics and losses due to intra-block correlations caused by the estimated interference statistics. The gain in adaptive processing (i.e., the reduction in the signal strength required to achieve specified false alarm and detection probabilities) is seen to be the ratio of the *AGI* to the change in the estimation and correlation losses from univariate to multivariate data.

Applications of the proposed detectors include any limited time duration signal in an interference background with moderately constrained stationarity conditions. The degree to which adaptive processing is applicable depends on the severity of the interference background. The *AGI*, which, for instance, is large for directions near to strong plane wave (isolated in arrival angle) interferences, must exceed the change in the estimation and correlation losses before adaptive processing becomes attractive.

2 ARRAY SIGNAL DETECTION BACKGROUND

The conventional detection of a signal arriving at an array of sensors from a particular direction may be viewed as two operations. First, the multivariate array data is processed to form a univariate *test statistic*. This is often accomplished by conventional beamforming and is discussed

in section 2.1. Second, a function, called the detector function or detector non-linearity, is applied to the univariate test statistic. The detector function is formed based on the statistical characteristics of the test statistic which are dependent on the statistical assumptions on the array data. The output of the detector function is then compared to a threshold to decide if a signal is present or not.

Adaptive array detectors form a detector function based on the statistical characteristics of multivariate array data rather than the univariate processed data. Unfortunately, this method is fraught with analysis and implementation difficulties. The estimation and inversion of the array data covariance matrix is typically required. As the number of array sensors increases, the matrix inversion becomes numerically inhibitive and the matrix estimation becomes statistically hazardous. A method of dealing with large arrays involves preprocessing the array data to a smaller dimension and then applying an adaptive detection algorithm. A very general matrix preprocessor is described in section 2.1, followed by a specific method, beam space preprocessing, that is applicable to adaptive detection. Common statistical models for the array data and the effects of the matrix preprocessing on these models are discussed in section 2.2.

2.1 Pre-Detector Signal Processing

The signal processing of an array of sensors in sonar or radar detection applications, as seen in figure 2-1, typically includes simultaneous time sampling of the continuous waveform at each of P sensors followed by transformation to the Fourier domain by a discrete Fourier transform (DFT). The frequency domain array data is beamformed to multiple angles with a signal detection algorithm at each beam output.

Beamforming is traditionally performed to increase the signal-to-noise ratio (SNR) prior to the detector by spatially filtering noise and interferences from other angles of arrival. This may be accomplished by using conventional, non-adaptive beamforming, or by data dependent, adaptive methods.

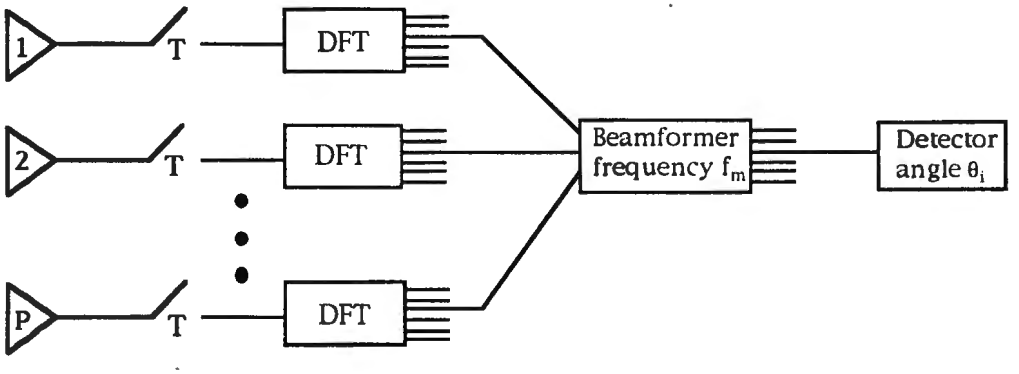

Figure 2-1 Typical signal processing of sensor arrays for detection.

A more general configuration of this system replaces the beamforming block with an angle dependent matrix preprocessor followed by a detector as seen in figure 2-2. If the array data for the m^{th} DFT bin and the l^{th} time snapshot is arranged in the P-by-1 vector,

$$\tilde{\mathbf{x}}_{ml} = [\tilde{x}_{1ml}\ \tilde{x}_{2ml} \cdots \tilde{x}_{Pml}]^T \tag{1}$$

and operated on by the P-by-N preprocessing matrix, $\mathbf{A}_{m\theta}$, the resulting N-by-1 preprocessed data vector is

$$\mathbf{x}_{ml} = \mathbf{A}_{m\theta}^H \tilde{\mathbf{x}}_{ml} \tag{2}$$

where the superscript ^{T} is the transpose operation and the superscript ^{H} is the conjugate transpose operation. Vectors are denoted by lower case bold letters, and matrices are denoted by upper case bold letters. The $\tilde{}$ notation found on vector variables indicates that the variable is at the array sensor level.

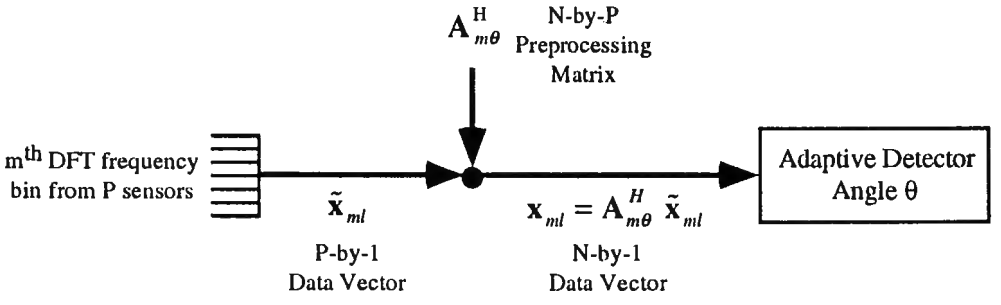

Figure 2-2 Preprocessing and adaptive detector.

Preprocessing the array sensor data provides N-dimensional data to the detector, where N is now dependent on the type of preprocessor employed. Conventional beamforming is represented by setting the matrix preprocessor to the array steering vector for the desired angle of arrival. Similarly, element space adaptive processing is represented by setting the matrix preprocessor to the P dimensional identity matrix, thus passing all of the sensor data to the detector. The matrix preprocessing structure also allows reduction of the adaptive dimension by transformations such that $1 < N < P$, as in the subarray and beamspace preprocessors discussed in [8].

Beamspace preprocessors, as seen in [8], are of particular interest because the adaptive dimension may be greatly reduced with minimal performance loss. For example, the AGI for an array with

$P = 64$ sensors using $N = 5$ beams in a beamspace preprocessor is typically within 0.5 dB of the fully adaptive beamformer AGI. The preprocessing matrix has the form

$$\mathbf{A}_{m\theta} = \left[\tilde{\mathbf{d}}_{m1}(\theta) \quad \ldots \quad \tilde{\mathbf{d}}_{mN}(\theta)\right], \tag{3}$$

where $\tilde{\mathbf{d}}_{mi}(\theta)$ represents an array steering vector at the m^{th} DFT frequency with a direction denoted by the index, i. The N beams that are chosen are those equally spaced in wavenumber and centered about the desired angle, θ.

When adaptive beamforming (and also detection) is employed, reduction of the adaptive dimension is crucial due to the numerical intensity of the implementation and the statistical hazards involved in the estimation of large covariance matrices. The reduced dimension adaptive techniques typically require estimation and inversion of an N-by-N covariance matrix at *each* DFT bin output. From a numerical computation and a statistical estimation standpoint this becomes difficult as N increases. Preprocessing the array data vectors to provide small N reduces numerical computations often with near equivalent average performance as shown by Owsley and Abraham [8] and also provides improved statistical performance as shown by Burgess and VanVeen [9].

2.2 Statistical Modeling

The array data vector from the m^{th} DFT frequency bin and the l^{th} time snapshot, $\tilde{\mathbf{x}}_{ml}$, is commonly modeled as a complex, P variate, Gaussian random vector. The following notation will be used throughout this paper to represent a P variate, complex Gaussian random vector with mean, μ, and covariance matrix, Σ:

$$\mathbf{x} \sim CN_P(\mu, \Sigma).$$

When no signal is present, denoted by the hypothesis H, the array data vector is distributed as

$$\tilde{\mathbf{x}}_{ml} | H \sim CN_P(\mathbf{0}, \tilde{\mathbf{Q}}_m), \tag{4}$$

where $\tilde{\mathbf{Q}}_m$ is the P-by-P covariance matrix representing the correlations between sensors at the m^{th} DFT frequency bin due to interference and noise.

There are two common signal models, the stochastic Gaussian signal with unknown power (SG) and the deterministic signal with unknown complex amplitude (SD). Both consider a plane wave

arrival with either stochastic or deterministic complex amplitude. For the SG case, the data vector is distributed as

$$\tilde{\mathbf{x}}_{ml}|K \sim CN_P(\mathbf{0}, s_{ml}\tilde{\mathbf{d}}_{m\theta}\tilde{\mathbf{d}}_{m\theta}^H + \tilde{\mathbf{Q}}_m) \tag{5}$$

where the hypothesis K represents signal present, $\tilde{\mathbf{d}}_{m\theta}$ represents the steering vector for the sensor level data and s_{ml} is the power of the signal in the m^{th} DFT bin and l^{th} time snapshot. The SD case, common in radar array processing, considers the time domain signal to be a sinusoid with known frequency and unknown complex amplitude, α_{ml}, yielding

$$\tilde{\mathbf{x}}_{ml}|K \sim CN_P(\alpha_{ml}\tilde{\mathbf{d}}_{m\theta}, \tilde{\mathbf{Q}}_m). \tag{6}$$

For comparison purposes, it will be assumed that the powers in the deterministic and Gaussian signals are the same, i.e.,

$$s_{ml} = |\alpha_{ml}|^2.$$

The data vectors are assumed to be independent, because of the Gaussian data assumption, for different frequencies and different time snapshots. Mathematically, this is described by

$$Cov[\tilde{\mathbf{x}}_{ml}\tilde{\mathbf{x}}_{nj}^H] = \delta_{mn}\delta_{lj}Cov[\tilde{\mathbf{x}}_{nl}\tilde{\mathbf{x}}_{nl}^H], \tag{7}$$

where δ_{ij}, the Kronecker delta function, is non-zero only when $i = j$ where it has unit value. The justification for this is based on [10] where, for the stationary continuous case, Hodgkiss and Nolte have shown that if the observation time of the signal is long enough, different Fourier coefficients become uncorrelated and, thus, are independent due to the Gaussian data assumption. It is also easily shown that similar results hold for the discrete case; that is, if the time series data is stationary, different DFT bins are approximately uncorrelated for a large enough DFT size and thus independent, assuming non-overlapping DFT's. Note that since our observation intervals are short, this places a minimum size constraint on the length of the DFT.

When the matrix preprocessing, described in section 2.1, is incorporated into the statistical description of the data, the SG and SD signals are respectively distributed as

$$\mathbf{x}_{ml}|K \sim CN_N(\mathbf{0}, s_{ml}\mathbf{d}_{m\theta}\mathbf{d}_{m\theta}^H + \mathbf{Q}_{m\theta}) \tag{8}$$

and

$$\mathbf{x}_{ml}|K \sim CN_N(\alpha_{ml}\mathbf{d}_{m\theta}, \mathbf{Q}_{m\theta}) \tag{9}$$

where the preprocessed steering vectors and interference covariance matrices are

$$\mathbf{d}_{m\theta} = \mathbf{A}_{m\theta}^H \tilde{\mathbf{d}}_{m\theta}$$

and

$$\mathbf{Q}_{m\theta} = \mathbf{A}_{m\theta}^H \tilde{\mathbf{Q}}_m \mathbf{A}_{m\theta}.$$

Due to the generality of the preprocessed data structure, the detection problem will be developed assuming that preprocessing has already been performed and, for notational convenience, suppress the dependence on the angle θ.

3 MAXIMUM LIKELIHOOD BASED ADAPTIVE DETECTORS

As previously mentioned, the array data is segmented in time into the PDB, containing interference and potentially signal, and the SDB, containing interference only. This structure, the statistical representation of the primary and secondary data, and its potential applications in the field of sonar are discussed in section 3.1. Then, following Robey's [5] derivation for the deterministic signal case, a detector for the Gaussian signal case is derived in section 3.2, and it is shown that each preprocessed array data vector in the PDB is used to form an adaptive beam output. The statistical distribution of the adaptive beam output is then described in section 3.3 for Gaussian and deterministic signals.

3.1 Array Data Structure

The primary-secondary data structure, commonly found in radar systems analysis, is composed of two sets of independent data blocks. Each data block is composed of a set of DFT bin outputs for multiple frequencies and time snapshots. The primary data block consists of data that is hypothesized to include signal energy. The secondary data block is independent of the PDB and must have the same interference statistics as that found in the primary data block at each frequency. The SDB is used to form estimates of the frequency dependent interference covariance matrix. This estimate is crucial to the constant false alarm rate (CFAR) property of the proposed detector. Figure 3-1 shows a typical contiguous primary and secondary data block set with M DFT frequencies, L time snapshots in the PDB, and J time snapshots in the SDB.

Each time snapshot-DFT frequency bin point in the data blocks represents a length N preprocessed data vector. Those in the SDB are assumed to contain no signal components, where those in the

PDB may. Statistically, the data vectors are described by equations (8) and (9), respectively, for the SG and SD cases. The no signal requirement of data vectors in the SDB implies that $s_{ml} = 0$ or $\alpha_{ml} = 0$. This yields the statistical representation

$$\mathbf{y}_{mj} \sim CN_N(\mathbf{0}, \mathbf{Q}_m) \tag{10}$$

for both signal types, where $\mathbf{y}_{mj}$ is the secondary data vector from the m^{th} DFT frequency and the j^{th} time snapshot (where $j = 1,\ldots,J$) and $\mathbf{Q}_m$ is the interference covariance matrix.

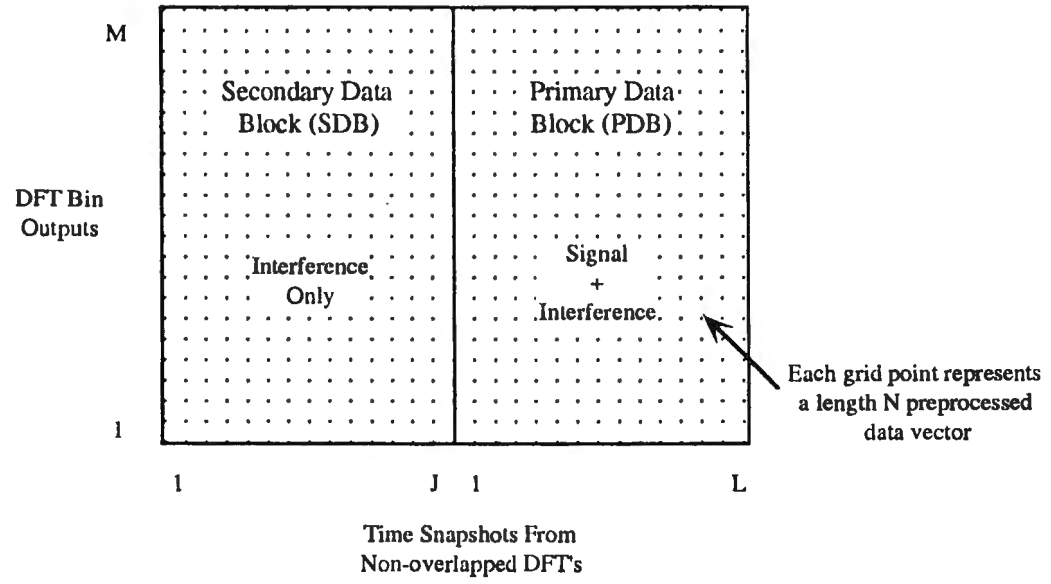

Figure 3-1 Primary and Secondary Data Block representation.

The SDB is not required to be a contiguous set of time snapshots. Windows leading and lagging the PDB may be used to estimate the interference covariance matrix, as in cell averaging CFAR systems, as long as steps are taken to insure that these windows are not contaminated by signal presence and have the same interference covariance structure as the PDB.

The most restricting requirement of this data structure lies in the required stationarity of the interference over both the primary and secondary data blocks. The detector performance is nearly optimal when the SDB contains a large number of time snapshots; this, however, conflicts with typical stationarity assumptions for sonar interferences. The requirement that the SDB not contain any energy due to the signal limits the application of this data structure to scenarios that have a definitive signal start or stop time.

The PDB must be sized based on the type of signal that is to be detected. Ideally, if the time-frequency characteristics of the signal were known exactly, only the cells that contained signal energy would be included in the PDB. However, since this information is rarely known and a detector that is robust against unknown signal time-frequency characteristics is desired, a block in time and frequency is utilized.

These restrictions on the PDB and SDB indicate that this data structure may be applied to limited time duration signals in a background that is stationary over some period of time greater than the length of the signal. Included in this category is the adaptive detection of an active sonar return with robustness against doppler, time and frequency spreading, and corrupted by reverberation that is stationary over both data blocks and spatially distinct from the desired signal.

This structure may also be applied to a signal that has a definitive onset but a long time duration. This type of signal suggests a sequential detector - this is not the focus of this memorandum, however, it may be a future research topic.

3.2 Detector Derivation

In the Neyman-Pearson sense of maximizing detection probability for a fixed false alarm rate, substituting the observed data into its likelihood ratio yields the optimal detector. When the statistical characterization of the data contains parameters with unknown values there is often no uniformly most powerful (UMP) test; that is, a single detector that provides optimal performance over all possible values of the unknown parameters. The GLRT often provides good (although suboptimal) performance when there are unknown parameters and no UMP test exists.

In the primary-secondary data structure problem, Kelly [4] has derived a GLRT detector for the single frequency deterministic signal case with a single time snapshot PDB. Robey et al. [5] and Chen and Reed [7] derived a test by forming a GLR statistic for the unknown complex signal amplitude assuming that the interference covariance matrix is known. The secondary data is then used to form the maximum likelihood estimate (MLE) of the interference covariance matrix, with the estimate substituted into the above GLR statistic. In this memorandum, a detector for the Gaussian signal case is developed following Robey et al. [5] and Chen and Reed [7], noting, as seen in [5], that the GLRT (i.e., Kelly [4]) has no assumed optimality over this method due to the nonexistence of a UMP test.

The GLRT requires maximization of the likelihood ratio, or equivalently, the log-likelihood ratio, with respect to the unknown signal powers, resulting in the test statistic

$$\lambda = \sum_{m,l} \max_{\{s_{ml}\}} \log\left[\frac{f_K\left(\mathbf{x}_{ml}|s_{ml},\mathbf{Q}_m\right)}{f_H\left(\mathbf{x}_{ml}|\mathbf{Q}_m\right)}\right], \tag{11}$$

where the summation indices m and l represent frequency and time snapshot in the PDB. The functions $f_i(\bullet)$ are the probability density functions (PDF's) of the primary data vectors under the null (H) and alternative (K) hypotheses for the Gaussian signal.

Substituting the N variate complex normal PDF's [11] for the Gaussian signal model and simplifying yields the form

$$\begin{aligned}\lambda_{SG} &= \sum_{m,l} \max_{s_{ml}} \log\left\{\frac{|\mathbf{Q}_m|}{\left|s_{ml}\mathbf{d}_m\mathbf{d}_m^H + \mathbf{Q}_m\right|}\exp\left[-\mathbf{x}_{ml}^H(s_{ml}\mathbf{d}_m\mathbf{d}_m^H + \mathbf{Q}_m)^{-1}\mathbf{x}_{ml} + \mathbf{x}_{ml}^H\mathbf{Q}_m^{-1}\mathbf{x}_{ml}\right]\right\} \\ &= \sum_{m,l} \max_{s_{ml}} \left\{\frac{s_{ml}\left|\mathbf{d}_m^H\mathbf{Q}_m^{-1}\mathbf{x}_{ml}\right|^2}{\left(1+s_{ml}\mathbf{d}_m^H\mathbf{Q}_m^{-1}\mathbf{d}_m\right)} - \log\left(1+s_{ml}\mathbf{d}_m^H\mathbf{Q}_m^{-1}\mathbf{d}_m\right)\right\}.\end{aligned} \tag{12}$$

Maximizing this form under the constraint that $s_{ml} \geq 0$ requires using the signal strength estimate

$$\hat{s}_{ml} = \begin{cases} \dfrac{1}{\mathbf{d}_m^H\mathbf{Q}_m^{-1}\mathbf{d}_m}\left[\dfrac{\left|\mathbf{d}_m^H\mathbf{Q}_m^{-1}\mathbf{x}_{ml}\right|^2}{\mathbf{d}_m^H\mathbf{Q}_m^{-1}\mathbf{d}_m} - 1\right] & T_{ml} \geq 1 \\ 0 & T_{ml} < 1 \end{cases} \tag{13}$$

where T_{ml} is the normalized adaptive beam output from the m^{th} DFT bin and the l^{th} time snapshot in the PDB; that is

$$T_{ml} = \frac{\left|\mathbf{d}_m^H\mathbf{Q}_m^{-1}\mathbf{x}_{ml}\right|^2}{\mathbf{d}_m^H\mathbf{Q}_m^{-1}\mathbf{d}_m}. \tag{14}$$

It is not expected that there will be signal energy in all cells of the PDB, so it is possible for the test statistic λ to be corrupted by non-signal cells. Intuitively, it seems that if there are a large number of non-signal cells in the PDB, performance may degrade. A method, attributed to Wolcin [1], for dealing with this problem is to form the MLE of the cell signal power under the constraint,

$$SIR_{ml} \geq \tau, \tag{15}$$

where the signal-to-interference ratio for the ml^{th} cell is defined as

$$SIR_{ml} = s_{ml}\mathbf{d}_m^H\mathbf{Q}_m^{-1}\mathbf{d}_m. \tag{16}$$

This technique essentially forms an estimate of where the signal lies in the time-frequency block of data; that is, if the estimated *SIR* is not greater than τ for a given cell then it is considered to have interference only and is not incorporated into the test statistic. Choosing $\tau = 0$ results in the conventional MLE for the unknown signal amplitude, since the *SIR* is zero if the signal power is zero. The effect on the signal power estimate of (13) is

$$\hat{s}_{ml} = \begin{cases} \dfrac{1}{\mathbf{d}_m^H\mathbf{Q}_m^{-1}\mathbf{d}_m}\left[\dfrac{\left|\mathbf{d}_m^H\mathbf{Q}_m^{-1}\mathbf{x}_{ml}\right|^2}{\mathbf{d}_m^H\mathbf{Q}_m^{-1}\mathbf{d}_m} - 1\right] & T_{ml} \geq 1+\tau \\ 0 & T_{ml} < 1+\tau \end{cases}. \tag{17}$$

Substituting this more general estimate back into (12) yields the detector statistic

$$\lambda_{SG} = \sum_{m,l} g_{SG}(T_{ml}), \tag{18}$$

where the SG detector nonlinearity has the following form:

$$g_{SG}(T) = \begin{cases} T - 1 - \log(T) & T \geq 1+\tau \\ 0 & T < 1+\tau \end{cases}. \tag{19}$$

Substituting the complex Gaussian PDF for the deterministic signal case into the log-likelihood ratio form of (11) yields

$$\lambda_{SD} = \sum_{ml} \max_{\{\alpha_{ml}\}} \mathbf{x}_{ml}^H\mathbf{Q}_m^{-1}\mathbf{x}_{ml} - \left(\mathbf{x}_{ml} - \alpha_{ml}\mathbf{d}_m\right)^H\mathbf{Q}_m^{-1}\left(\mathbf{x}_{ml} - \alpha_{ml}\mathbf{d}_m\right). \tag{20}$$

By completing the square in terms of α_{ml}, it is seen that choosing

$$\hat{\alpha}_{ml} = \frac{\mathbf{d}_m^H \mathbf{Q}_m^{-1} \mathbf{x}_{ml}}{\mathbf{d}_m^H \mathbf{Q}_m^{-1} \mathbf{d}_m}$$

will maximize the log-likelihood ratio to

$$\begin{aligned} \lambda_{SD} &= \sum_{ml} \frac{\left| \mathbf{d}_m^H \mathbf{Q}_m^{-1} \mathbf{x}_{ml} \right|^2}{\mathbf{d}_m^H \mathbf{Q}_m^{-1} \mathbf{d}_m} \\ &= \sum_{ml} g_{SD}(T_{ml}) \end{aligned}, \tag{21}$$

where the deterministic signal detector non-linearity is actually the linear function

$$g_{SD}(T) = T. \tag{22}$$

This is commonly known as an energy detector and has been explored for a single frequency, single PDB time snapshot case by Robey [5], Chen and Reed [7], and for a time domain implementation by Baggenstoss and Kay [12].

Substituting the MLE of the interference covariance matrix at the m^{th} DFT frequency over the secondary data block at each frequency,

$$\hat{\mathbf{Q}}_m = \frac{1}{J} \sum_{j=1}^{J} \mathbf{y}_{mj} \mathbf{y}_{mj}^H, \tag{23}$$

into the adaptive beam output (14) yields

$$\hat{T}_{ml} = \frac{\left| \mathbf{d}_m^H \hat{\mathbf{Q}}_m^{-1} \mathbf{x}_{ml} \right|^2}{\mathbf{d}_m^H \hat{\mathbf{Q}}_m^{-1} \mathbf{d}_m}. \tag{24}$$

3.3 Statistical Description of the Adaptive Beam Output

The adaptive beam output (24) formed by using the MLE of the interference covariance matrix is used in both the SG and SD detectors. In order to calculate the thresholds required to implement the detectors and to analyze their performance, the probability density function of the adaptive beam output needs to be determined. The approach used is to first determine the density function of the adaptive beam output conditioned on the interference covariance matrix estimate for the Gaussian and deterministic signals. The next step is to statistically describe the parameters of these

conditional distributions that depend on the estimated covariance matrix. The randomness introduced by estimating the interference covariance matrix may be described by two independent scalar random variables, the foundation of which comes from the work of Reed, Mallett, and Brennan [3], and is shown in Appendix A.

The adaptive beam output, conditioned on the interference covariance matrix estimate, is the magnitude squared of a univariate complex Gaussian random variable. As a general case, consider the N-variate complex Gaussian random vector

$$\mathbf{x} \sim CN_N(\mu, \Sigma),$$

and the form

$$T = \left|\mathbf{w}^H \mathbf{x}\right|^2, \tag{25}$$

for some constant vector $\mathbf{w}$. The temporary variable, $Z = \mathbf{w}^H \mathbf{x}$, has the density function of a univariate complex Gaussian random variable, i.e.,

$$Z \sim CN\left(\mathbf{w}^H \mu, \mathbf{w}^H \Sigma \mathbf{w}\right).$$

The magnitude squared of Z, which is equivalent to (25), is the sum of the squares of two independent Gaussian random variables with the same variance. This sum is proportional to a non-central Chi-squared random variable with two degrees of freedom. Thus, when appropriately scaled by the constant κ, (25) is distributed as

$$Y = \frac{1}{\kappa} T \sim \chi_2^2(\zeta),$$

which has probability density function [13]

$$f_Y(y) = \frac{1}{2}\exp\left(-\frac{y+\zeta}{2}\right) I_0\left(\sqrt{y\zeta}\right) \qquad y > 0,$$

where $I_0(\bullet)$ is a modified Bessel function of zero order. The scale and non-centrality parameters are, in this case,

$$\kappa = \frac{\mathbf{w}^H \Sigma \mathbf{w}}{2}$$

and

$$\zeta = 2\frac{\left|\mathbf{w}^H \mu\right|^2}{\mathbf{w}^H \Sigma \mathbf{w}}. \tag{26}$$

The mean and power of the adaptive beam output, T, in terms of the scale and non-centrality parameters, are

$$E[T] = \kappa(2+\zeta)$$

and

$$E\left[T^2\right] = \kappa^2\left(\zeta^2 + 8\zeta + 8\right). \tag{27}$$

The adaptive beam output (24) may be written as in (25) by letting

$$\mathbf{w} = \frac{\hat{\mathbf{Q}}_m^{-1}\mathbf{d}_m}{\sqrt{\mathbf{d}_m^H \hat{\mathbf{Q}}_m^{-1}\mathbf{d}_m}}. \tag{28}$$

By substituting (28) and the mean and covariance from equation (8) or (9) into equations (26) and (27) it is seen that the chi-squared scale and non-centrality parameters and the adaptive beam output mean and power may be written as functions of the following two *independent* Gamma and Beta distributed random variables:

$$r_m = \frac{\mathbf{d}_m^H \mathbf{Q}_m^{-1}\mathbf{d}_m}{\mathbf{d}_m^H \hat{\mathbf{Q}}_m^{-1}\mathbf{d}_m} \sim Gamma(J-N+1, 1/J)$$

and

$$\rho_m = \frac{\left(\mathbf{d}_m^H \hat{\mathbf{Q}}_m^{-1}\mathbf{d}_m\right)^2}{\left(\mathbf{d}_m^H \hat{\mathbf{Q}}_m^{-1}\mathbf{Q}_m \hat{\mathbf{Q}}_m^{-1}\mathbf{d}_m\right)\left(\mathbf{d}_m^H \mathbf{Q}_m^{-1}\mathbf{d}_m\right)} \sim Beta(J-N+2, N-1). \tag{29}$$

The density functions for the Gamma and Beta random variables and the derivation of these results are found in Appendix A.

Utilizing the statistical descriptions of the Gaussian (8) and deterministic signals (9), the scale, non-centrality, mean and power of the respective adaptive beam outputs are as shown in table 3-1. In considering the results found in table 3-1, it is seen that the Gaussian signal case always results in a central Chi-square distribution, which, with two degrees of freedom, is the exponential

distribution. The deterministic signal case results in the exponential distribution only when the *SIR* is zero, i.e. when no signal is present. The conditional mean of the adaptive beam output is identical for both signal types. The power for the SD case is always less than or equal to that of the SG case with equality only when the *SIR* is zero. The only dependence of the scale and non-centrality parameters, that describe the conditional distribution of the adaptive beam output, on the true interference covariance matrix, is through the *SIR* as defined in (16). When no signal is present, the *SIR* is zero and the adaptive beam output distribution is free from dependence on the interference covariance matrix. Thus, any detector based on the adaptive beam output will have a constant false alarm rate.

Table 3-1 Scale, non-centrality, mean and power for the adaptive beam output from the ml^{th} cell in the PDB for Gaussian and deterministic signals.

Signal	Scale κ	Non-centrality ζ	Mean $E[T_{ml}]$	Power $E[T_{ml}^2]$
SG	$\frac{1+\rho_m SIR_{ml}}{2\rho_m r_m}$	0	$\frac{1+\rho_m SIR_{ml}}{\rho_m r_m}$	$2\frac{(1+\rho_m SIR_{ml})^2}{(\rho_m r_m)^2}$
SD	$\frac{1}{2\rho_m r_m}$	$2\rho_m SIR_{ml}$	$\frac{1+\rho_m SIR_{ml}}{\rho_m r_m}$	$2\frac{(1+\rho_m SIR_{ml})^2}{(\rho_m r_m)^2} - \frac{SIR_{ml}^2}{r_m^2}$

It is useful to consider how the Gamma and Beta random variables change with the dimension of the data, N, and the size of the secondary data block, J. When $N=1$ the beamspace matrix preprocessor is performing conventional beamforming and it is seen that the Beta random variable becomes degenerate at one; that is, $\rho=1$ with probability one. The secondary data is thus used to estimate the unknown conventional beam output power and then used to normalize the primary data as in cell averaging CFAR systems. This is a realistic, implementable, non-adaptive detector. If, additionally, the size of the SDB goes to infinity, which is not a practical assumption, both the Gamma and Beta random variables become degenerate at one. This situation represents infinite time averaging of the unknown interference covariance matrix which is equivalent to perfect knowledge about the interference structure. This case is known as the *ideal conventional detector* because of the assumed knowledge of the interference statistics at the beam output level. These results are summarized in table 3-2.

Table 3-2 Gamma and Beta random variables under certain N and J.

N	J	Gamma RV	Beta RV
$N>1$	$N<J<\infty$	r_{ml}	ρ_{ml}
$N=1$	$N<J<\infty$	r_{ml}	$\rho_{ml}=1$
$N=1$	$J\to\infty$	$r_{ml}\to 1$	$\rho_{ml}\to 1$

4 DETECTOR ANALYSIS

In section 3, detectors were derived based on Gaussian and deterministic signal assumptions. The resulting detectors were expressed as the summation, over all DFT frequency - time snapshot cells in the PDB, of a univariate statistic, the adaptive beam output, evaluated at a detector non-linearity. The detection statistic is

$$\lambda = \sum_{ml} g_i(T_{ml}) \qquad (30)$$

where $g_i(\bullet)$ represents the detector non-linearity. When the number of cells in the PDB is large enough, a central limit theorem (CLT) based approximation to a Gaussian random variable may be used to analyze the performance of these detectors. This requires knowledge of the mean and variance of the test statistic, λ, under the no-signal hypothesis (H) and the signal-present hypothesis (K). The time-frequency characteristics of the signal have not been restricted in deriving the detectors. But, in order to make analysis tractable, certain restrictions need to be placed on the strength and time-frequency location of the signal in the PDB.

The signal restrictions and the mean and variance of the detector test statistics are respectively described in sections 4.1 and 4.2. The detector performance analysis using the CLT approximation is described in section 4.3.

4.1 Signal Time-Frequency Model

Without some simplification of the signal model, the analysis of the detectors, in particular the variance computation, is difficult due to the correlation between adaptive beam outputs, at the same DFT frequency, introduced by the estimated interference covariance matrix. A model that provides some freedom in the placement of signal energy in the cells of the PDB is desired. First, it is assumed that when the signal is present in a time-frequency cell, it will have a constant *SIR*. Next, the number of time snapshot cells that have signal present, for a particular DFT frequency, is either

zero or L_s. The number of DFT frequencies that contain L_s *signal* cells will be M_s. Thus, the total number of signal cells is $M_s L_s$ and we define the fraction of signal cells to total cells to be

$$\gamma = \frac{M_s L_s}{ML}. \tag{31}$$

This is graphically described in figure 4-1 with an example where $L_s = 3$, $M_s = 9$, $L = 7$, and $M = 14$. The positioning of the DFT frequencies that contain signal and the signal cells at those DFT frequencies is not restricted.

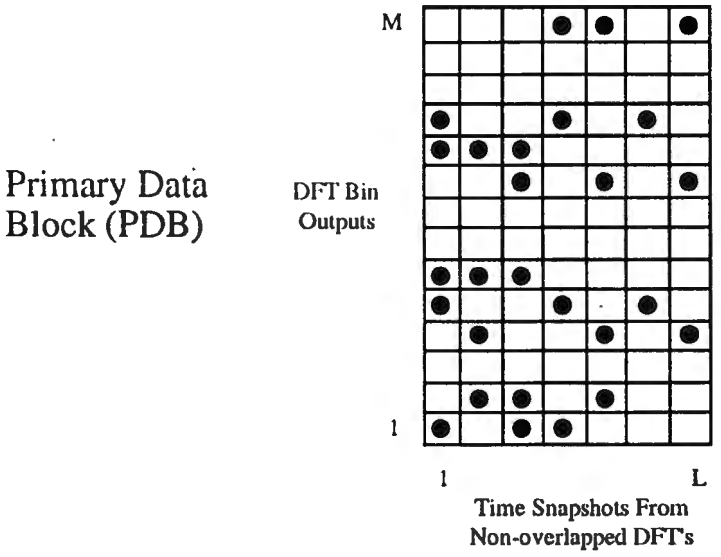

Figure 4-1 Graphical representation of signal time-frequency location. Signal is present in 3 of 7 time snapshot cells ($L_s = 3$, $L = 7$) for 9 of 14 DFT frequencies ($M_s = 9$, $M = 14$).

4.2 Test Statistic Mean and Variance

The SG and SD detector functions were derived in section 3. In this section the performance of the SG detector for the Gaussian signal and the SD detector for both the Gaussian and deterministic signal, as depicted in figure 4-2, are analyzed.

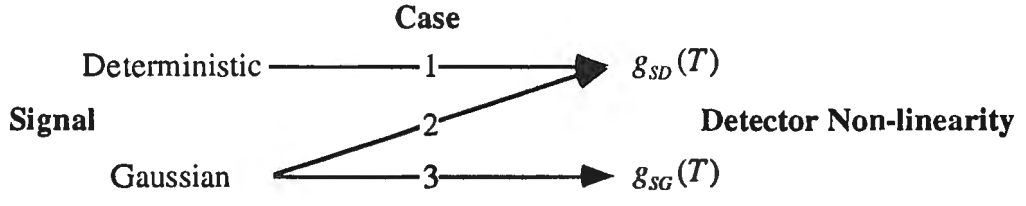

Figure 4-2 Signal and detector descriptions for analysis cases.

The block level mean and variance (i.e., mean and variance of (30)) under the signal present hypothesis (K) may be found in terms of the previously described signal time-frequency parameters and the mean and variance of the detector non-linearity, $g_i(\bullet)$, operating on a single adaptive beam output, T, with no signal and with a signal with a specified SIR. These expressions are given by

$$E_K[\lambda] = ML\{(1-\gamma)E_0[g_i(T)] + \gamma E_{SIR}[g_i(T)]\}$$

and

$$\begin{aligned} Var_K[\lambda] = {} & ML(1-\gamma)Var_0[g_i(T)] + ML\gamma\, Var_{SIR}[g_i(T)] \\ & + ML[L-1+\gamma(L_s-2L+1)]\left(h(0,0) - E_0[g_i(T)]^2\right) \\ & + 2ML\gamma(L-L_s)\left(h(0,SIR) - E_0[g_i(T)]E_{SIR}[g_i(T)]\right) \\ & + ML\gamma(L_s-1)\left(h(SIR,SIR) - E_{SIR}[g_i(T)]^2\right), \end{aligned} \tag{32}$$

where the subscript on the expectation terms on the right hand sides of the equations denote the SIR for the cell creating the adaptive beam output, T. The term on the second line in the variance is due to the correlation between the adaptive beam outputs at the same frequency. The intermediate function, $h(a,b)$, is defined as

$$h(a,b) = E[g_i(T_a)g_i(T_b)], \tag{33}$$

where T_a and T_b are adaptive beam outputs formed from the *same* interference covariance matrix estimate and two independent primary data vectors with signal to interference ratio equal to a and b respectively. The mean and variance under the no signal hypothesis (H) may be found by setting $\gamma = 0$ and $L_s = 0$ in (32), i.e.,

$$\begin{aligned} E_H[\lambda] &= ML\,E_0[g_i(T)] \\ Var_H[\lambda] &= ML\,Var_0[g_i(T)] + ML(L-1)\left(h(0,0) - E_0[g_i(T)]^2\right) \end{aligned} \tag{34}$$

Thus we only need to evaluate the cell level mean and variance (i.e., the mean and variance of the detector non-linearity) and the function $h(a,b)$ in order to determine the detector performance. Closed forms exist for the SD detector for both signal types and are shown in table 4-1. As expected, the only difference between the two signal types is that the variance of the adaptive beam output for the deterministic signal is less than that for the Gaussian signal.

The r and ρ random variables in table 4-1 are, respectively, Gamma and Beta distributed, as discussed in section 3.3, and have closed form inverse moments when $J > N+1$. The required inverse moments are

$$E[r^{-1}] = \frac{J}{J-N}, \qquad E[r^{-2}] = \frac{J^2}{(J-N)(J-N-1)},$$
$$E[\rho^{-1}] = \frac{J}{J-N+1}, \qquad E[\rho^{-2}] = \frac{J(J-1)}{(J-N)(J-N+1)} . \qquad (35)$$

Table 4-1 Cell level mean, variance and $h(a,b)$ function for the deterministic signal detector operating on deterministic and Gaussian signals.

Deterministic Signal Detector		
Parameter	**Deterministic Signal**	**Gaussian Signal**
$E_{SIR}[T]$	$E[r^{-1}]\{SIR + E[\rho^{-1}]\}$	$E[r^{-1}]\{SIR + E[\rho^{-1}]\}$
$Var_{SIR}[T]$	$\{SIR + E[\rho^{-1}]\}^2\{2E[r^{-2}] - E[r^{-1}]^2\}$ $+2E[r^{-2}]\{E[\rho^{-2}] - E[\rho^{-1}]^2 - \frac{1}{2}SIR^2\}$	$\{SIR + E[\rho^{-1}]\}^2\{2E[r^{-2}] - E[r^{-1}]^2\}$ $+2E[r^{-2}]\{E[\rho^{-2}] - E[\rho^{-1}]^2\}$
$h_{SD}(a,b)$	$E[r^{-2}]\{ab + (a+b)E[\rho^{-1}] + E[\rho^{-2}]\}$	$E[r^{-2}]\{ab + (a+b)E[\rho^{-1}] + E[\rho^{-2}]\}$

Due to the non-linear form of the Gaussian signal detector, the analysis is considerably more difficult and is done only for the Gaussian signal case. By utilizing the conditional distribution of the adaptive beam output, reducing the expectation over the Gamma random variable, and using the transformation $u = \frac{1+\tau}{T}$, the i^{th} moment of the SG detector non-linearity may be expressed as

$$E_{SIR}[g_{SG}^i(T)] = E_{\rho u}\left[\frac{(J-N+1)\rho(1+\tau)g_{sg}^i\left(\frac{1+\tau}{u}\right)}{Ju^2(1+\rho SIR)\left[1+\frac{\rho(1+\tau)}{Ju(1+\rho SIR)}\right]^{J-N+2}}\right], \qquad (36)$$

where ρ is Beta distributed as previously described and u is a uniform random variable (independent of ρ) with density function

$$f(u) = 1 \qquad 0 \le u \le 1. \qquad (37)$$

The function $h(a,b)$ may similarly be expressed as

$$h_{SG}(a,b) = E_{\rho u v}\left[\frac{(J-N+1)(J-N+2)\rho^2(1+\tau)^2 g_{SG}\left(\frac{1+\tau}{u}\right)g_{SG}\left(\frac{1+\tau}{v}\right)}{J^2u^2v^2(1+\rho a)(1+\rho b)\left[1+\frac{\rho}{J}\left(\frac{1+\tau}{u(1+\rho u)}+\frac{1+\tau}{v(1+\rho b)}\right)\right]^{J-N+3}}\right], \qquad (38)$$

where both u and v are independent uniform random variables with the density function described in (37). In reducing the expectation over the Gamma random variable, the following two relationships are used:

$$E_r[re^{r\theta}] = \frac{J-N+1}{J(1-\theta/J)^{J-N+2}}$$

and

$$E_r[r^2e^{r\theta}] = \frac{(J-N+1)(J-N+2)}{J^2(1-\theta/J)^{J-N+3}}. \qquad (39)$$

The evaluation of these functions would require two- and three-dimensional integrals for each *SIR*. Therefore, Monte-Carlo integration is used with the uniform and Beta random variables generated only once. The concept of Monte-Carlo integration is discussed in Appendix B.

4.3 Detection Performance via CLT

In order to implement and evaluate the detector, a threshold must be chosen based on the desired false alarm probability. The false alarm probability is the probability of the test statistic crossing some threshold, l, when no signal is present; that is,

$$P_{FA} = \Pr\{\lambda \geq l|H\}. \qquad (40)$$

Since the test statistic is approximated by a Gaussian distributed random variable with mean and variance as described in (34) when no signal is present, the threshold that provides the specified false alarm performance may be written as

$$l = E_H[\lambda] - \Phi^{-1}(P_{FA})\sqrt{Var_H[\lambda]}, \qquad (41)$$

where the function $\Phi(\bullet)$ is the standard Gaussian cumulative distribution function, defined by

$$\Phi(x) = \Pr\{Z \leq x\} = \int_{z=-\infty}^{x} \frac{1}{\sqrt{2\pi}} e^{-\frac{z^2}{2}} dz, \qquad (42)$$

and the superscript $^{-1}$ represents a functional inverse.

The probability of detecting a signal is the probability that the test statistic crosses a threshold (set by the desired false alarm rate) when the signal is present, i.e.,

$$P_D = \Pr\{\lambda \geq l | K\}. \tag{43}$$

Using the CLT normal approximation once again, the probability of detection is

$$P_D = \Phi\left(\frac{E_K[\lambda] - l}{\sqrt{Var_K[\lambda]}}\right). \tag{44}$$

The derivation of these forms for the threshold and probability of detection is straightforward and is found in Nuttall [2].

The detection probability is dependent on the false alarm probability, the *SIR* found in each signal cell, the total number of cells containing signal, the signal location parameters previously discussed, the adaptive dimension, and the fixed sizes of the PDB and SDB. Here, the *SIR* required to achieve desired false alarm *and* detection probabilities is considered. Clearly, the *SIR* enters into the detection probability through the mean and variance of (32), however, not in a simple fashion. In general, the *SIR* required to achieve specified detection and false alarm probabilities may be found numerically by evaluating (44) until the desired detection probability is found. The SG detector requires this approach, however, the closed form solution to the mean and variance for the SD detector provides an exact solution. As seen in table 4-1, the cell level mean, variance, and $h(a,b)$ functions for the SD detector are either first or second order polynomials in *SIR*. The block level mean and variance are linear combinations of these terms and may be written, respectively, as a monomial and a quadratic in *SIR* as follows:

$$E_K[\lambda] = m_1 SIR + m_0,$$

where

$$m_1 = ML\gamma E\left[r^{-1}\right]$$

$$m_0 = ML\, E\left[r^{-1}\right] E\left[\rho^{-1}\right]'$$

and

$$Var_K[\lambda] = a_2 SIR^2 + a_1 SIR + a_0,$$

where

$$a_2 = ML\gamma\left\{U_S E\left[r^{-2}\right] + L_s\left(E\left[r^{-2}\right] - E\left[r^{-1}\right]^2\right)\right\}$$
$$a_1 = 2ML\gamma E\left[\rho^{-1}\right]\left\{(L+1)E\left[r^{-2}\right] - LE\left[r^{-1}\right]^2\right\}$$
$$a_0 = ML^2\left\{E\left[r^{-2}\right]E\left[\rho^{-2}\right] - E\left[r^{-1}\right]^2 E\left[\rho^{-1}\right]^2\right\} + ML\,E\left[r^{-2}\right]E\left[\rho^{-2}\right] \tag{45}$$

The Boolean variable,

$$U_S = \begin{cases} 1 & SG \\ 0 & SD \end{cases},$$

represents the difference between the Gaussian and deterministic signals.

For the SD detector, we can express the equality (44) in the form

$$\Phi^{-1}(P_D)\sqrt{Var_K[\lambda]} = E_K[\lambda] - l. \tag{46}$$

Following Nuttall [2], we solve this by squaring both sides, which yields a quadratic form in *SIR*, i.e.,

$$b_2 SIR^2 + b_1 SIR + b_0 = 0,$$

where

$$b_2 = m_1^2 - a_2\left[\Phi^{-1}(P_D)\right]^2$$
$$b_1 = 2m_1(m_0 - l_{SD}) - a_1\left[\Phi^{-1}(P_D)\right]^2, \tag{47}$$
$$b_0 = (m_0 - l_{SD})^2 - a_0\left[\Phi^{-1}(P_D)\right]^2$$

where the threshold for the SD detector may be written as

$$l_{SD} = m_0 - \sqrt{a_o}\,\Phi^{-1}(P_{FA}). \tag{48}$$

The quadratic formula yields the solution to (47), however, only one root will satisfy the transcendental equation (46). Notice that the above coefficients depend on the square of $\Phi^{-1}(P_D)$, thus, removing dependence on the sign. As in [2], the sign of $\Phi^{-1}(P_D)$ is used in the quadratic formula to yield the correct root, that is,

$$SIR = \frac{-b_1 + sign\left(\Phi^{-1}(P_D)\right)\sqrt{b_1^2 - 4b_2 b_0}}{2b_2}. \tag{49}$$

The $sign\left(\Phi^{-1}(P_D)\right)$ term in the result may be explained by allowing P_D to increase slightly from one half, which causes $\Phi^{-1}(P_D)$ to increase slightly from zero, thus at $P_D = 0.5$, the roots of the quadratic are the same. An increased P_D requires more SIR, thus we want the larger root which is achieved in (49) when $b_2 > 0$, which is true in the neighborhood of $P_D = 0.5$.

As is seen in Nuttall [2], this method may also be applied to solving for the signal coverage parameter, γ, required to achieve desired detection and false alarm probabilities using the ideal conventional detector for a fixed SIR. This is done to facilitate plotting the required SIR against the signal coverage parameter. The SG detector requires substantial computation to evaluate the required SIR for each value of γ. This method, conversely, computes the cell level mean and variance and finds the value of γ that yields the desired performance, only requiring the numerical integration of two equations for each SIR.

The ideal conventional detector represents perfect knowledge of the conventional beam output power which causes the $h(a,b)$ function (33) to become

$$h_{Ideal}(a,b) = E_a\left[g_i(T_a)\right]E_b\left[g_i(T_b)\right], \tag{50}$$

because there is no correlation between adaptive beam outputs at the same DFT frequency (the term due to correlation in the block level variance (32) thus goes to zero). Substituting the ideal conventional detector mean and variance into the transcendental equation (46) yields the quadratic form in the signal coverage parameter, γ, i.e.,

$$c_2\gamma^2 + c_1\gamma + c_0 = 0,$$

where

$$\begin{aligned} c_2 &= ML\left\{E_{SIR}\left[g_i(T)\right] - E_0\left[g_i(T)\right]\right\}^2 \\ c_1 &= 2\sqrt{MLVar_0\left[g_i(T)\right]}\,\Phi^{-1}(P_{FA})\left\{E_{SIR}\left[g_i(T)\right] - E_0\left[g_i(T)\right]\right\} \\ &\quad -\left[\Phi^{-1}(P_D)\right]^2\left\{Var_{SIR}\left[g_i(T)\right] - Var_0\left[g_i(T)\right]\right\} \\ c_0 &= Var_0\left[g_i(T)\right]\left\{\left[\Phi^{-1}(P_{FA})\right]^2 - \left[\Phi^{-1}(P_D)\right]^2\right\} \end{aligned} \tag{51}$$

As before, the solution is the quadratic formula with a sign correction, that is,

$$\gamma = \frac{-c_1 + sign\left(\Phi^{-1}(P_D)\right)\sqrt{c_1^2 - 4c_2c_0}}{2c_2} \quad . \tag{52}$$

5 DETECTOR PERFORMANCE

In previous sections, Gaussian and deterministic signal detectors were developed and a method of determining the *SIR* required to achieve specified detection and false alarm probabilities was provided. In section 5.1, the *SIR* is factored into an ideal case with covariance matrix estimation losses and intra-block correlation losses in order to determine what has the most effect on the required *SIR*. It is seen that the detector gain due to adaptive processing is related to the *AGI*. In section 5.2, the *AGI* for Owsley's standard test case [14] is shown, as well as the average loss due to beam space matrix preprocessing. In section 5.3, the ideal conventional detector *SIR* is examined against the fraction of cells containing signal, γ, for the SD detector with Gaussian and deterministic signals and for the SG detector with various *SIR* thresholds operating on a Gaussian signal. Estimation and correlation losses are then considered for various size secondary and primary data blocks and adaptive dimension. From these plots, the *SIR* required to achieve desired detection and false alarm probabilities can be determined.

5.1 SIR Decomposition

It is known that estimating the unknown interference covariance matrix causes performance degradation compared to the perfect knowledge or clairvoyant detector. These losses may be categorized as an estimation loss and as a correlation loss. The correlation loss results from using the same estimated covariance matrix for each time snapshot in the PDB at each DFT frequency. Analytically, this is represented by factoring the *SIR* into the amount of *SIR* required for an ideal conventional detector, SIR_{Ideal}, with a loss due to estimation of the interference covariance matrix, E_{Loss}, and a loss due to the intra-block correlations, C_{Loss}; that is,

$$SIR_{Rqd} = SIR_{Ideal} E_{Loss} C_{Loss}, \tag{53}$$

where the estimation and correlation losses are greater than or equal to one. The ideal conventional detector is a detector operating at the output of a conventional beamformer when the beam output power is known.

The required cell level signal power, s_{Rqd}, may be written, utilizing the definition of the *SIR*, as

$$s_{Rqd} = s_{Ideal}\left(\frac{E_{Loss}C_{Loss}}{AGI(N)}\right), \tag{54}$$

where s_{Ideal} is the required cell level signal power for the ideal conventional detector for a given interference structure and $AGI(N)$ represents the AGI achieved using the P by N preprocessing matrix, $\mathbf{A}_{m\theta}$. Thus,

$$\begin{aligned} AGI(N) &= \left(\mathbf{d}_{m\theta}^{H}\mathbf{Q}_{m\theta}^{-1}\mathbf{d}_{m\theta}\right)\left(\tilde{\mathbf{d}}_{m}^{H}\tilde{\mathbf{Q}}_{m}\tilde{\mathbf{d}}_{m}\right) \\ &= \tilde{\mathbf{d}}_{m}^{H}\mathbf{A}_{m\theta}\left(\mathbf{A}_{m\theta}^{H}\tilde{\mathbf{Q}}_{m}\mathbf{A}_{m\theta}\right)^{-1}\mathbf{A}_{m\theta}^{H}\tilde{\mathbf{d}}_{m}\left(\tilde{\mathbf{d}}_{m}^{H}\tilde{\mathbf{Q}}_{m}\tilde{\mathbf{d}}_{m}\right). \end{aligned} \tag{55}$$

The loss due to estimation of the interference statistics is defined as the ratio of the required SIR for a detector where no correlation loss occurs ($L=1$, with M fixed) to that of the ideal conventional detector; that is,

$$E_{Loss}(J,N) = \frac{SIR_{Rqd}(J,N,L=1)}{SIR_{Ideal}}. \tag{56}$$

The correlation loss is defined as the ratio of the worst case required SIR (in terms of L_s) for the given detector parameters to that of a detector where no correlation loss occurs; that is,

$$C_{Loss}(J,N,L) = \frac{\max\limits_{\{L_s\}} SIR_{Rqd}(J,N,L,L_s)}{SIR_{Rqd}(J,N,L=1)}. \tag{57}$$

The gain in adaptive processing over conventional may be expressed as the ratio of their required signal powers, i.e.,

$$\begin{aligned} Gain &= \frac{s_{Rqd}(N=1)}{s_{Rqd}(N)} \\ &= AGI(N)\left(\frac{E_{Loss}(J,N=1)}{E_{Loss}(J,N)}\right)\left(\frac{C_{Loss}(J,N=1,L)}{C_{Loss}(J,N,L)}\right), \end{aligned} \tag{58}$$

noting that $AGI(N=1)=1$. To improve over the implementable conventional detector, the AGI need only be greater than the change in the estimation and correlation losses.

5.2 Typical AGI

As described in (55) and applied in (58), the *AGI* represents the potential improvement when adaptive processing is utilized and is a function of the interference covariance matrix and the matrix preprocessing. In order to provide some measure of what typical *AGI* values are, Owsley's standard test case (STC) [14] is analyzed for beam space preprocessing on a half wavelength linearly spaced 64 sensor array. This test case consists of five plane wave signals amidst two angularly extended signals. In figure 5-1, the expected conventional and adaptive beam responses to Owsley's STC, Scenario 1, are shown. Any signal arriving from a direction other than the look direction is considered to be an interference.

In figure 5-2, the *AGI* achieved using element space adaptive processing is shown as a function of the direction of arrival (DOA) of the signal. The largest *AGI* values are located close in arrival angle to the strong plane wave interferences and are seen to be greater than 10 dB. In figure 5-3, the average, over arrival angles, of the loss in *AGI* incurred by the beamspace preprocessing is plotted against the adaptive dimension of the preprocessor (number of beams used in the preprocessing matrix). This curve provides an idea of how much *AGI* is lost due to beamspace preprocessing. In this example, five beams provides an average of 0.5 *dB* of loss.

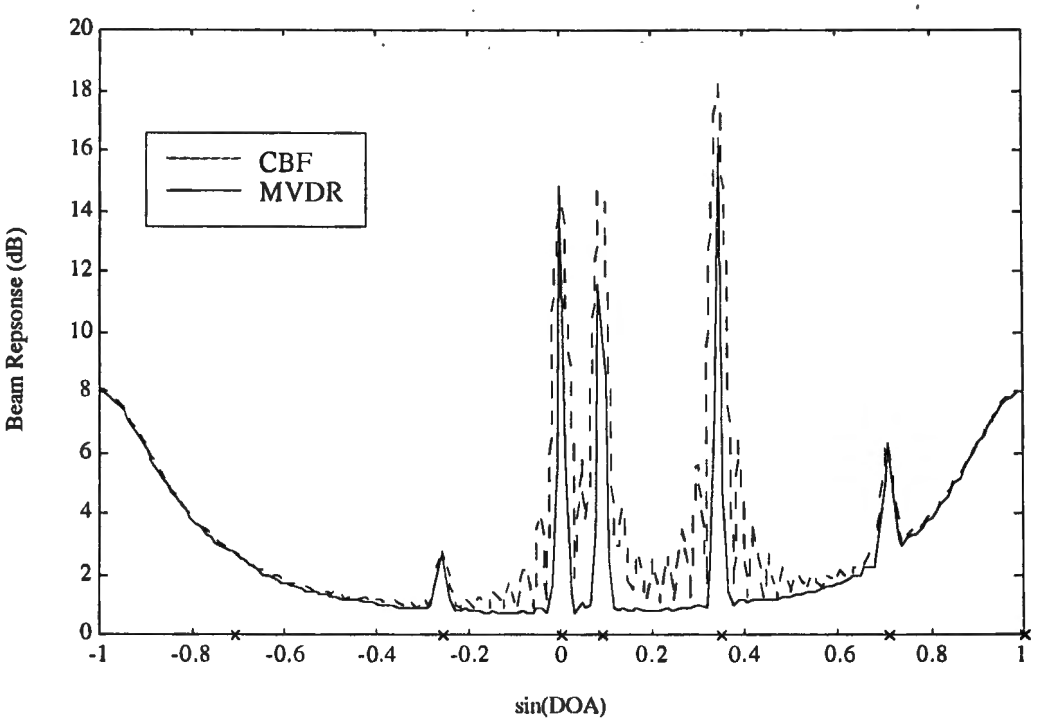

Figure 5-1 Expected conventional and adaptive beam responses to Owsley's STC, Scenario 1, for a half wavelength, linearly spaced, 64 sensor array. The marks on the abscissa indicate signal placement.

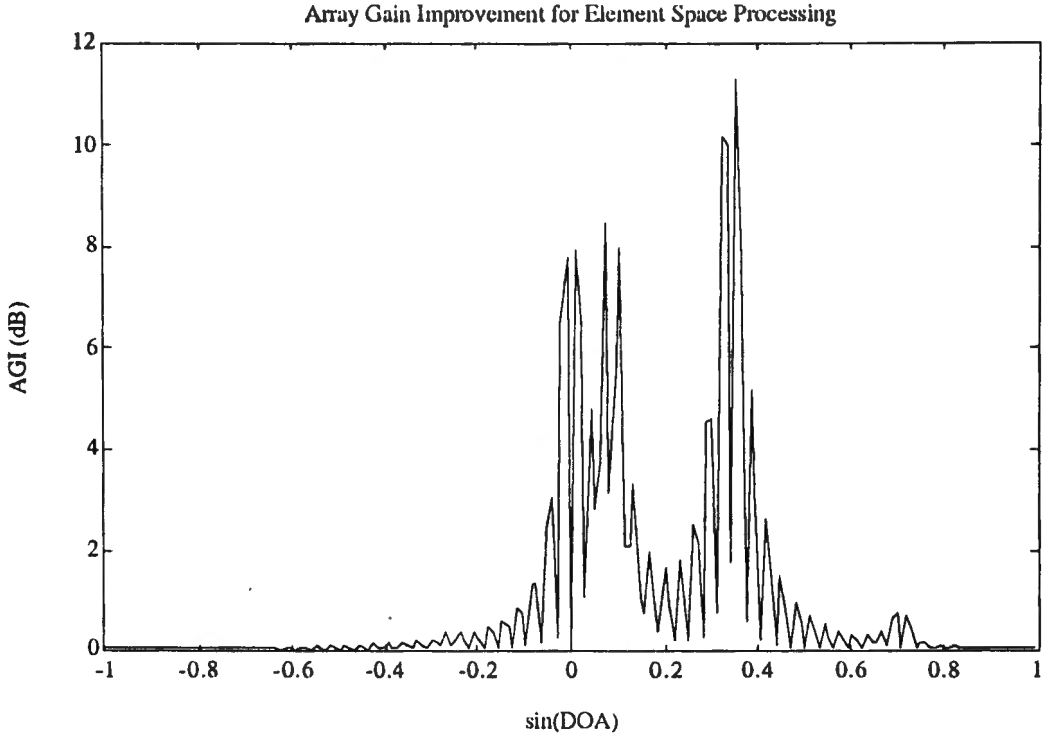

Figure 5-2 Array gain improvement (*AGI*) for Owsley's STC, Scenario 1, for element space processing of a half wavelength, linearly spaced, 64 sensor array.

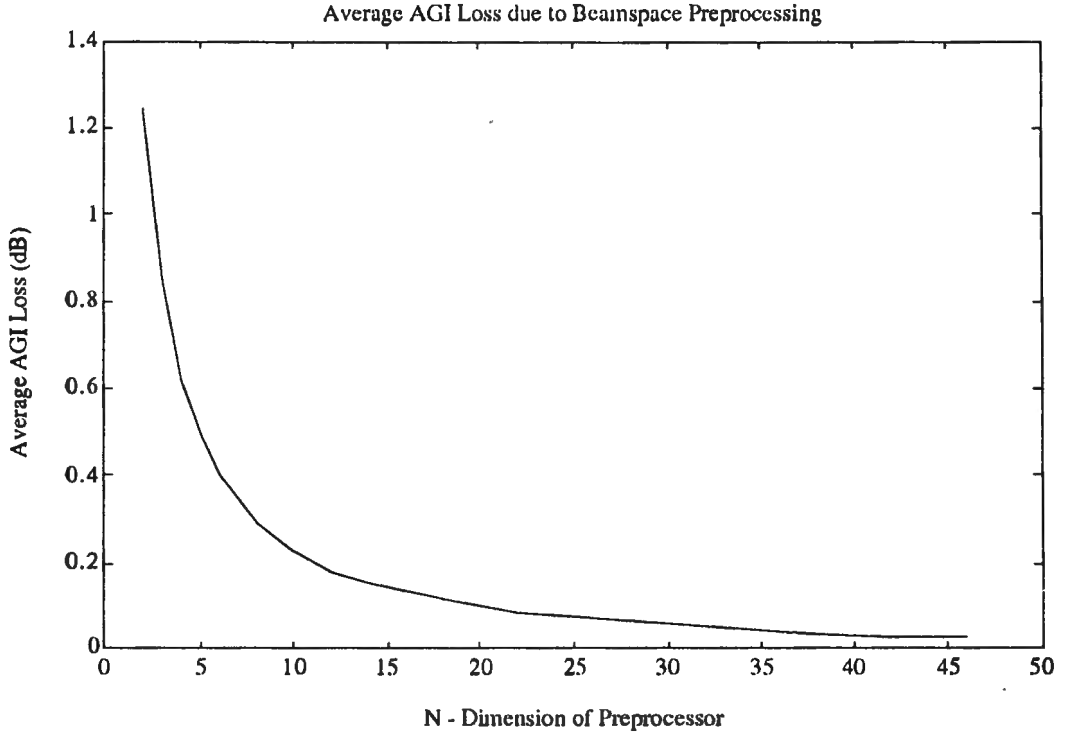

Figure 5-3 Average loss in *AGI* compared to element space adaptive processing for Owsley's STC, Scenario 1, due to beamspace preprocessing as a function of the number of beams used in the preprocessor, for a half wavelength, linearly spaced, 64 sensor array.

5.3 Performance Results

The method of analysis for the SD and SG detectors used here will first consider the *SIR* required to achieve specified detection and false alarm probabilities for the ideal conventional detector against the parameter γ, the fraction of cells in the PDB that contain signal. The estimation loss is then determined for a narrowband (γ near zero) and a broadband (γ near one) signal, with changing SDB sizes and adaptive dimensions. Finally, the correlation loss is determined as a function of the PDB size for a fixed SDB size. Throughout this analysis, the total number of cells in the PDB, ML, is held constant. The SD detector is considered for both the deterministic and Gaussian signals. The SG detector is considered only for the Gaussian signal. These signal-detector combinations will be denoted by: $SD-SD$, $SG-SD$, and $SG-SG$, with the first variable representing the signal type and the second the detector type.

The SIR required to achieve a $P_D = 0.9$ and $P_{FA} = 10^{-3}$, for an ideal conventional detector with $ML = 1024$, is shown in figure 5-4 for the $SD-SD$ and $SG-SD$ combinations and for the $SG-SG$ combination with $\tau = 0, 2,$ and 4. This plot corresponds to those found in [2] for the Gaussian signals.

For small γ signals, i.e. signals that are confined to very few cells in the PDB, the SG detector performs better with increasing threshold, τ. Raising the threshold too high, thus decreasing the number of non-zero values in (18), violates the assumptions required to use the CLT in the analysis for small γ signals. At values of γ close to unity, i.e. signals that almost completely cover the PDB, the SD outperforms all of the SG detectors for the Gaussian signals. This characteristic is expected and has been shown before (see [2]). An intuitive rationale is that the deterministic signal should be easier to detect than the Gaussian signal because the signal structure is known exactly. This is demonstrated in figure 5-4 for the SD detector with the most degradation for the Gaussian signal when γ is small.

When the interference statistics are unknown and need to be estimated, the increase in the required *SIR* is quantified by the $E_{Loss}(J,N)$ metric. For a fixed number of PDB cells ($ML = 1024$), this parameter is considered against increasing values of SDB size (J), for $N = 1, 5, 10,$ and 15 for both small γ and large γ signals. Figures 5-5 and 5-6, respectively, show the estimation loss for the $\gamma = 0.1$ and $\gamma = 0.9$ signals. The ideal conventional detector required *SIR* is noted in figure 5-4 for both of these signal cases. Recall that the number of time snapshots in the PDB is one ($L = 1$) so there is no loss due to correlation.

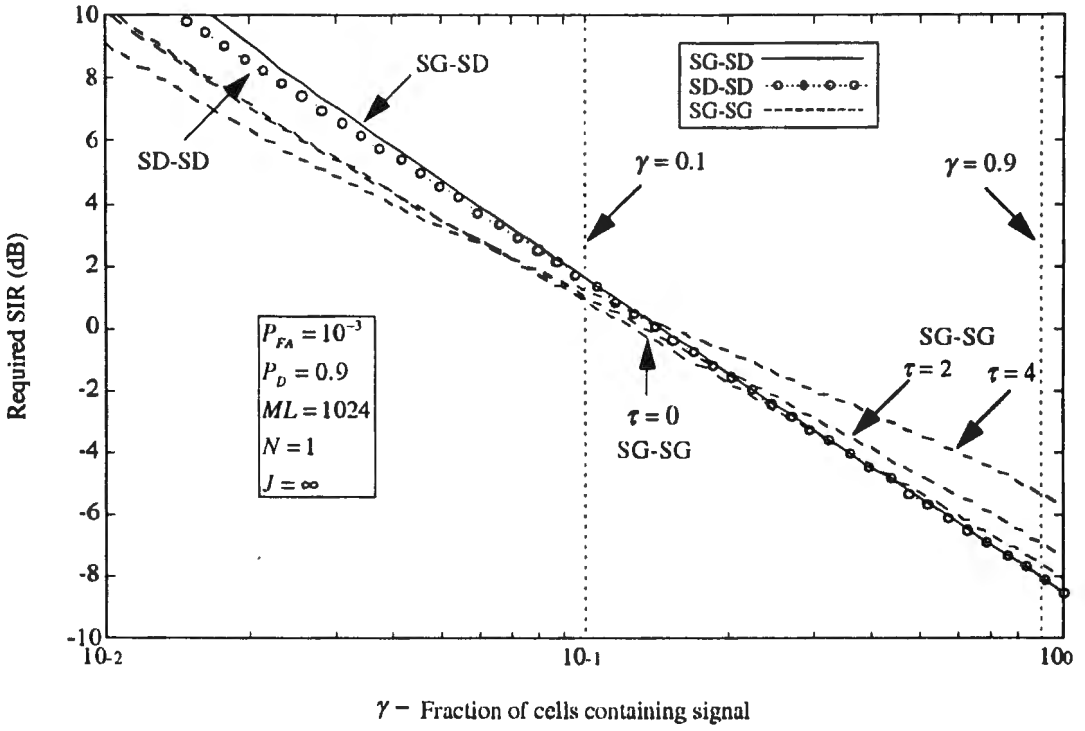

Figure 5-4 SIR_{Ideal} vs. γ for $ML = 1024$, $P_D = 0.9$, and $P_{FA} = 10^{-3}$.

As expected, the loss due to estimating the interference statistics decreases as the size of the SDB is increased. The estimation loss seems invariant to γ for the $SD-SD$ and $SG-SD$ combinations, with the loss nearly indistinguishable for the two signal types. The SG detector ($\tau = 0$) shows increased loss for small γ, with a higher sensitivity for larger N. Note also that the losses for each detector are approximately the same for the large γ signal.

In order to consider the loss due to correlation of the normalized beam output statistics, $C_{Loss}(J,N,L)$, we choose a particular size for the SDB ($J = 20$). In most cases, the SDB size will be dictated by the stationarity of the interference, thus this is a reasonable specification. Figures 5-7 and 5-8 show the loss in required SIR due to correlation against the PDB size (L) for $N = 1, 5, 10,$ and 15 and respectively for the $\gamma = 0.1$ and $\gamma = 0.9$ signals, respectively.

The correlation losses for all the signal-detector combinations increase as the number of time snapshots in the PDB increases. As with the estimation loss, the loss for the $SD-SD$ and SG D combinations are indistinguishable. The correlation loss is also seen to be larger for the small γ signal for all the signal-detector combinations and slightly sensitive to larger N.

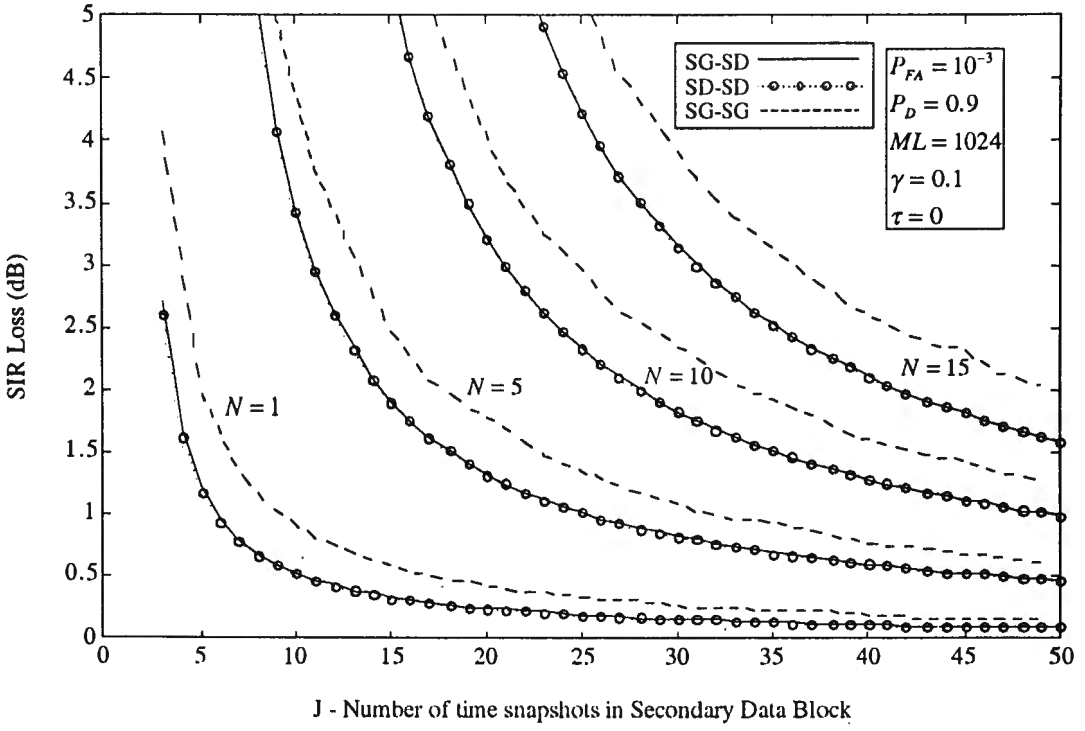

Figure 5-5 $E_{Loss}(J,N)$ vs. J for $\gamma = 0.1$, $ML = 1024$, $P_D = 0.9$, and $P_{FA} = 10^{-3}$.

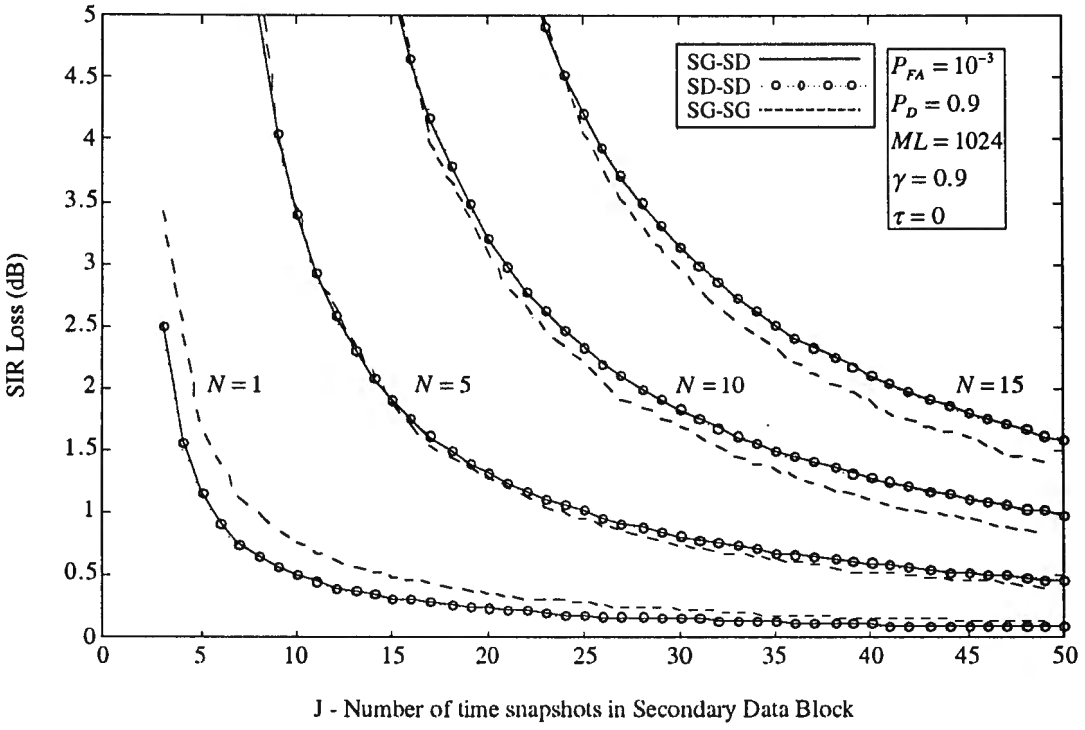

Figure 5-6 $E_{Loss}(J,N)$ vs. J for $\gamma = 0.9$, $ML = 1024$, $P_D = 0.9$, and $P_{FA} = 10^{-3}$.

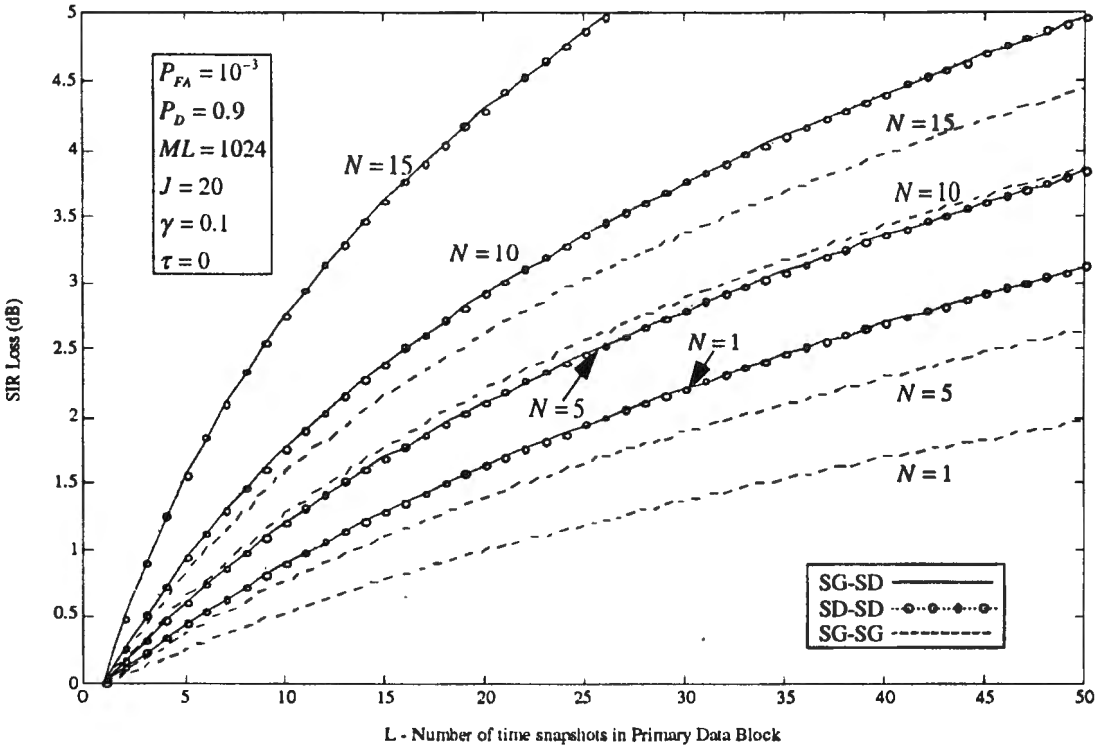

Figure 5-7 $C_{Loss}(J,N,L)$ vs. L for $J = 20$, $\gamma = 0.1$, $ML = 1024$, $P_D = 0.9$, and $P_{FA} = 10^{-3}$.

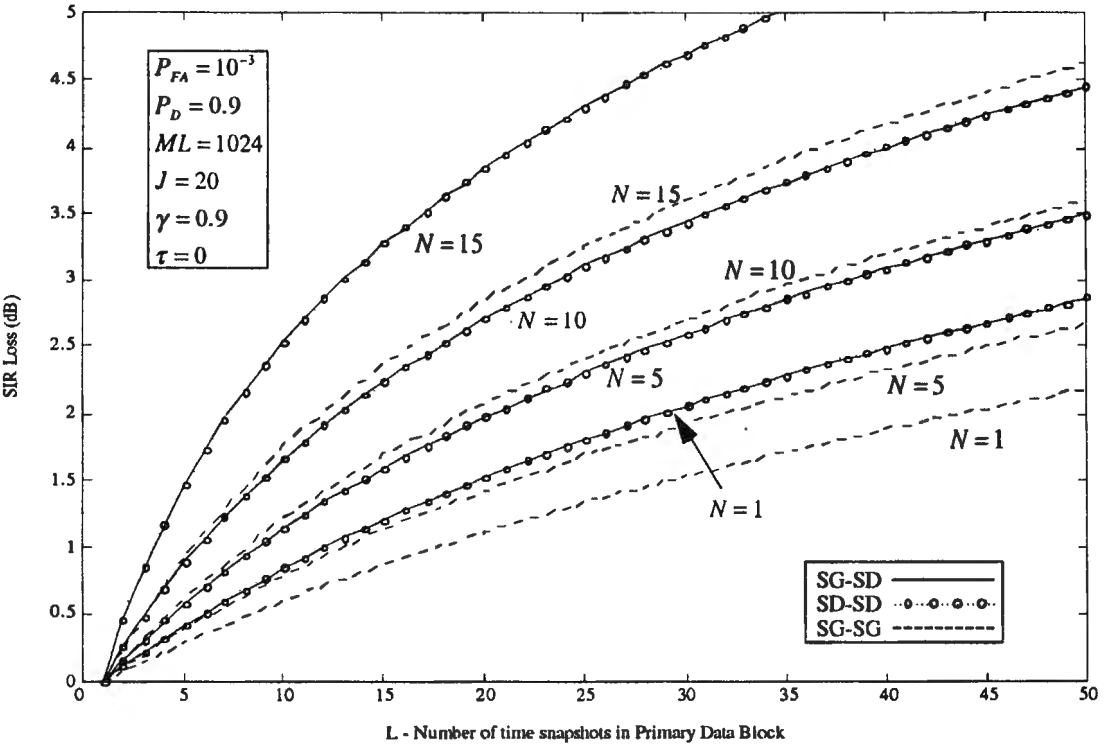

Figure 5-8 $C_{Loss}(J,N,L)$ vs. L for $J = 20$, $\gamma = 0.9$, $ML = 1024$, $P_D = 0.9$, and $P_{FA} = 10^{-3}$.

6 CONCLUSIONS

This memorandum considers the utilization of multiple sensor array data in the adaptive detection of sonar and radar signals. The signal processing prior to the detector, including a dimension reducing matrix preprocessor and statistical models commonly used to describe the data, were introduced as a preface to the adaptive detector development. Detectors were then developed for the Gaussian and deterministic signal cases, where signal energy is restricted to a block in time and frequency, the primary data block (PDB). The Gaussian signal detector was derived allowing the signal-to-interference ratio (*SIR*) that is observed at each time snapshot-DFT frequency cell in the PDB to be thresholded. This imparts a robust character to the detector against diverse time-frequency characteristics of a received signal. A second block, disjoint in time from the block containing the signal, is used to estimate the interference statistics which are common to both blocks. Applications of this data structure include active sonar returns and limited time duration signals that are corrupted by interference that is stationary over both data blocks.

The detection and false alarm probabilities of the detectors were then determined using a central limit theorem based approximation to a normal random variable. Closed form solutions were found for the deterministic signal detector operating on both the deterministic and Gaussian signals. The Gaussian signal detector required the evaluation of multi-dimensional integrals which was accomplished by a Monte-Carlo method.

The performance of the detectors was then described by the cell level *SIR* required to achieve specified detection and false alarm probabilities. The *SIR* was factored into the *SIR* required for an ideal conventional detector affected by an estimation loss and an intra-block correlation loss. When the matrix preprocessing of the array data provides the detector with multivariate data, an adaptive processing gain, quantified by the array gain improvement (*AGI*), may counter the estimation and correlation losses. The *AGI* increases with the dimension of the preprocessed data, when beamspace preprocessing is used, however, this improvement is opposed by an increase in the estimation and correlation losses. The estimation loss decreases as the time length of the block used to estimate the interference statistics increases. The correlation loss increases with the time length of the block containing the signal. Both the estimation and correlation losses are seen to increase with the adaptive dimension of the detectors.

These results lead to a desired detector structure that has (i) a large time block used to estimate the interference statistics, (ii) a small time block that contains the signal, (iii) a small adaptive dimension to reduce estimation and correlation losses, and (iv) a large adaptive dimension to improve the *AGI*. Clearly, (iii) and (iv) are conflicting requirements, however, the adaptive dimension may be reduced substantially using beam space preprocessing with a loss in *AGI* that is

easily countered by the reduced estimation and correlation losses. The large time desired for estimation of the interference statistics, (i), is opposed by the limited stationarity of typical sonar interferences. The size of the time block containing signal is determined by the type of signal being detected and by the size of the DFT that decorrelates the time series data. Fewer time snapshots in the block containing signal is desired which requires a larger DFT which is good for decorrelating the time series, however it also means fewer time snapshots in the block used to estimate the interference statistics, thus increasing the estimation loss. The decrease in correlation loss, however, is not enough to offset the increase in estimation loss, thus the DFT size should be chosen large enough to decorrelate the time series data and small enough to provide adequate estimation of the interference statistics.

This memorandum proposes two adaptive detector structures based on deterministic and Gaussian signals that exist in a limited region in time and frequency. The detectors estimate and then employ the unknown interference covariance matrix which results in a constant false alarm rate detector. A method for system level design is provided by evaluating the effect of the size of the primary (signal and interference) and secondary (interference only) data blocks on the *SIR* required to achieve specified performance for several adaptive dimensions. The size of the DFT, the type of signal to be detected, and the length of the stationarity of the interference affect these sizes, and, thus, the estimation and correlation losses incurred on the required *SIR*. Balancing these losses is the gain due to adaptive processing which increases with the adaptive dimension of the preprocessing. Coupling the estimation and correlation losses with the adaptive processing gain, as a function of the adaptive dimension, an optimal choice of adaptive dimension is possible for a given interference environment.

APPENDIX A - PDF OF CFAR AND SIR LOSS RANDOM VARIABLES

The distribution of the adaptive beam output for the m^{th} DFT frequency and the l^{th} time snapshot in the PDB (24) conditioned on the estimate of the interference covariance matrix was described in terms of *SIR* loss and CFAR loss parameters. The *SIR* loss parameter, was first derived and shown to be Beta distributed by Reed, Mallet and Brennan [3]; its definition and distribution are

$$\rho_m = \frac{\left(\mathbf{d}_m^H \hat{\mathbf{Q}}_m^{-1} \mathbf{d}_m\right)^2}{\left(\mathbf{d}_m^H \hat{\mathbf{Q}}_m^{-1} \mathbf{Q}_m \hat{\mathbf{Q}}_m^{-1} \mathbf{d}_m\right)\left(\mathbf{d}_m^H \mathbf{Q}_m^{-1} \mathbf{d}_m\right)},$$

$$\rho_m \sim Beta(J-N+2, N-1),$$

and

$$f_\rho(\rho) = \frac{\Gamma(J+1)}{\Gamma(J-N+2)\Gamma(N-1)} \rho^{J-N+1}(1-\rho)^{N-2} \qquad 0<\rho<1, \qquad \text{(A-1)}$$

where the Gamma function is defined as

$$\Gamma(z) = \int_{x=0}^{\infty} x^{z-1} e^{-x} dx.$$

For positive integer values of z, the Gamma function is

$$\Gamma(z) = (z-1)! \qquad z = 1,2,3,...$$

In this appendix, it will be shown that the CFAR loss parameter is a Gamma distributed random variable and that it is statistically independent from the *SIR* loss parameter. As seen in (29), the CFAR loss parameter is defined by

$$r_m = \frac{\mathbf{d}_m^H \mathbf{Q}_m^{-1} \mathbf{d}_m}{\mathbf{d}_m^H \hat{\mathbf{Q}}_m^{-1} \mathbf{d}_m}. \qquad \text{(A-2)}$$

It is now convenient to introduce the complex Wishart distribution of $J\hat{\mathbf{Q}}_m$:

$$\mathbf{A} = J\hat{\mathbf{Q}}_m \sim CW_N(J, \mathbf{Q}_m). \qquad \text{(A-3)}$$

Equation (A-3) reads: the N-by-N matrix $\mathbf{A}$ has a complex Wishart distribution with J degrees of freedom and scale matrix $\mathbf{Q}_m$. Letting $\mathbf{v} = \mathbf{Q}_m^{-\frac{1}{2}} \mathbf{d}_m$, the CFAR loss parameter becomes

$$r_m = \frac{\mathbf{v}^H\mathbf{v}}{J\,\mathbf{v}^H\mathbf{Q}_m^{\frac{1}{2}}\mathbf{A}^{-1}\mathbf{Q}_m^{\frac{1}{2}}\mathbf{v}}. \tag{A-4}$$

Letting $\mathbf{B} = \mathbf{Q}_m^{-\frac{1}{2}}\mathbf{A}\mathbf{Q}_m^{-\frac{1}{2}}$ and $\mathbf{u} = \frac{\mathbf{v}}{\sqrt{\mathbf{v}^H\mathbf{v}}}$ (so that $\mathbf{u}^H\mathbf{u} = 1$), then

$$r_m = \frac{1}{J\,\mathbf{u}^H\mathbf{B}^{-1}\mathbf{u}}. \tag{A-5}$$

Let $\mathbf{u} = \mathbf{P}^H\mathbf{e}_1$ and $\mathbf{C} = \mathbf{P}\mathbf{B}\mathbf{P}^H$, where $\mathbf{P}$ is orthogonal $\left(\mathbf{P}^H\mathbf{P} = \mathbf{I}\right)$ and $\mathbf{e}_1$ is the first unit vector (i.e. $\mathbf{e}_1 = [1\cdots 0]^T$), giving

$$r_m = \frac{1}{J\,\mathbf{e}_1^H\mathbf{C}^{-1}\mathbf{e}_1}. \tag{A-6}$$

Now it is seen that $\mathbf{C}$ is a Wishart distributed matrix by using the property that if $\mathbf{A} \sim CW_N(J,\Sigma)$ and $\mathbf{M}$ is L-by-N with rank L, then $\mathbf{M}\mathbf{A}\mathbf{M}^H \sim CW_L\left(J,\mathbf{M}\Sigma\mathbf{M}^H\right)$. This is found for the real Wishart matrix in Muirhead [15] and is easily extended to the complex Wishart case. Thus writing $\mathbf{C}$ as

$$\mathbf{C} = \mathbf{P}\mathbf{Q}_m^{-\frac{1}{2}}\mathbf{A}\mathbf{Q}_m^{-\frac{1}{2}}\mathbf{P}^H,$$

it is seen to be complex Wishart distributed,

$$\begin{aligned}\mathbf{C} &\sim CW_N\left(J,\mathbf{P}\mathbf{Q}_m^{-\frac{1}{2}}\mathbf{Q}_m\mathbf{Q}_m^{-\frac{1}{2}}\mathbf{P}^H\right)\\ &\sim CW_N(J,\mathbf{I})\end{aligned}. \tag{A-7}$$

In this same fashion, the *SIR* loss parameter may be written as

$$\rho_m = \frac{\left(\mathbf{e}_1^H\mathbf{C}^{-1}\mathbf{e}_1\right)^2}{\mathbf{e}_1^H\mathbf{C}^{-2}\mathbf{e}_1}. \tag{A-8}$$

Proceeding, we first partition the matrix $\mathbf{C}$ and $\mathbf{D} = \mathbf{C}^{-1}$ as follows:

$$\mathbf{C} = \begin{bmatrix} c_{11} & \mathbf{c}_{12}^H \\ \mathbf{c}_{21} & \mathbf{C}_{22} \end{bmatrix}$$

and

$$\mathbf{D} = \mathbf{C}^{-1} = \begin{bmatrix} d_{11} & \mathbf{d}_{12}^{H} \\ \mathbf{d}_{21} & \mathbf{D}_{22} \end{bmatrix}, \tag{A-9}$$

where c_{11} and d_{11} are scalars, $\mathbf{C}_{22}$ and $\mathbf{D}_{22}$ are $(N-1)$-by-$(N-1)$ matrices, and the other dimensions follow accordingly. Now, clearly,

$$\mathbf{e}_1^{H}\mathbf{C}^{-1}\mathbf{e}_1 = d_{11}$$

and

$$\mathbf{e}_1^{H}\mathbf{C}^{-2}\mathbf{e}_1 = d_{11}^2 + \mathbf{d}_{12}^{H}\mathbf{d}_{21}.$$

Either from equating $\mathbf{CD} = \mathbf{I}$ or from the Matrix Theory Appendix of [15],

$$d_{11} = \left(c_{11} - \mathbf{c}_{12}^{H}\mathbf{C}_{22}^{-1}\mathbf{c}_{21}\right)^{-1}$$

and

$$\begin{aligned} \mathbf{d}_{21} &= \frac{-\mathbf{C}_{22}^{-1}\mathbf{c}_{21}}{c_{11} - \mathbf{c}_{12}^{H}\mathbf{C}_{22}^{-1}\mathbf{c}_{21}}. \\ &= -d_{11}\mathbf{C}_{22}^{-1}\mathbf{c}_{21} \end{aligned} \tag{A-10}$$

The complex Wishart matrix form of a theorem found in Muirhead ([15] p.93 Thm. 3.2.10) is now required. The extension from the real Wishart matrix form is simply performed by following Muirhead's proof and using the complex Wishart distributional information found in [11].

Theorem - Suppose that $\mathbf{A} \sim CW_N(J,\Sigma)$, with the partitions

$$\mathbf{A} = \begin{bmatrix} \mathbf{A}_{11} & \mathbf{A}_{12} \\ \mathbf{A}_{21} & \mathbf{A}_{22} \end{bmatrix} \quad \text{and} \quad \Sigma = \begin{bmatrix} \Sigma_{11} & \Sigma_{12} \\ \Sigma_{21} & \Sigma_{22} \end{bmatrix},$$

where A_{11} and Σ_{11} are M-by-M matrices. Now define

$$A_{11\cdot 2} = A_{11} - A_{12}A_{22}^{-1}A_{21}$$

and

$$\Sigma_{11\cdot 2} = \Sigma_{11} - \Sigma_{12}\Sigma_{22}^{-1}\Sigma_{21},$$

then

(*i*) $\mathbf{A}_{11\cdot 2} \sim CW_M\left(J - N + M, \Sigma_{11\cdot 2}\right)$

(*ii*) $\mathbf{A}_{11\cdot 2}$ is independent of $\mathbf{A}_{12}$ and $\mathbf{A}_{22}$

Now, letting $M = 1$, $A = C$, and $\Sigma = I$ in the above theorem, it is seen that

$$\mathbf{e}_1^H \mathbf{C}^{-1} \mathbf{e}_1 = (\mathbf{C}_{11\cdot 2})^{-1}$$

and

$$\mathbf{e}_1^H \mathbf{C}^{-2} \mathbf{e}_1 = \left(1 + \mathbf{c}_{12}^H \mathbf{C}_{22}^{-2} \mathbf{c}_{21}\right)(\mathbf{C}_{11\cdot 2})^{-2}. \tag{A-11}$$

Substituting these into (A-6) and (A-8) yields

$$r_m = \frac{\mathbf{C}_{11\cdot 2}}{J}$$

and

$$\rho_m = \frac{1}{1 + \mathbf{c}_{12}^H \mathbf{C}_{22}^{-2} \mathbf{c}_{21}}. \tag{A-12}$$

Utilizing the above theorem, it is seen that r_m and ρ_m are independent and that the distribution of $\mathbf{C}_{11\cdot 2} = J r_m$ is $CW_1(J - N + 1, 1)$, which is a $Gamma(J - N + 1, 1)$ distribution, thus r_m is distributed as

$$r_m \sim Gamma(J - N + 1, 1/J),$$

with PDF

$$f_r(r) = \frac{J^{J-N+1}}{\Gamma(J - N + 1)} r^{J-N} e^{-Jr} \qquad r > 0. \tag{A-13}$$

APPENDIX B - MONTE-CARLO INTEGRATION

It is very difficult to evaluate higher dimension integrals numerically [16]. To avoid this problem, Monte-Carlo integration [16] is employed for evaluating the two and three dimensional integrals in this report. This method involves writing the integral as the expectation of a function over a set of (in this case) independent random variables,

$$\Psi = \int g(\mathbf{x}) dF(\mathbf{x}) = E_{\mathbf{x}}[g(\mathbf{x})], \qquad \text{(B-1)}$$

where $g(\mathbf{x})$ is the function to be integrated and $F(\mathbf{x})$ is the joint cumulative distribution function of the random vector $\mathbf{x}$.

The integral is then approximated by forming a large number of these random variables and computing the sample mean of the desired function,

$$\hat{\Psi} = \frac{1}{N}\sum_{n=1}^{N} g(\mathbf{x}_n), \qquad \text{(B-2)}$$

where the $\mathbf{x}_n$ are independent samples of the random vector $\mathbf{x}$. This is known to converge in probability to the true value of the integral as the number of samples used tends to infinity.

REFERENCES

[1] Wolcin, J.J., Personal Notes, 1983.

[2] Nuttall, A.H., "Required Signal-to-Noise Ratios for Maximum Likelihood Detection of Transient Signals," NUSC TM-891140, 29 August 1989.

[3] Reed, I.S., J.D. Mallet, and L.E. Brennan, "Rapid Convergence Rate in Adaptive Arrays," IEEE Trans. on Aerospace and Electronic Systems, Vol. AES-10, No. 6, pp.853-863, November 1974.

[4] Kelly, E.J., "An Adaptive Detection Algorithm," IEEE Trans. on Aerospace and Electronic Systems, Vol. AES-22, No. 1, pp.115-127, March 1986.

[5] Robey, F.C., D.R. Furhmann, E.J. Kelly, and R. Nitzberg, "A CFAR Adaptive Matched Filter Detector," IEEE Trans. on Aerospace and Electronic Systems, Vol. 28, No. 1, pp.208-216, January 1992.

[6] Robey, F.C., "A Covariance Modeling Approach to Adaptive Beamforming and Detection," Lincoln Laboratory Tech. Rpt. 918, 30 July 1991.

[7] Chen, W.S. and I.S. Reed, "A New CFAR Detection Test for Radar," in *Digital Signal Processing I*, pp.198-214, Academic Press, 1991.

[8] Owsley, N.L. and D.A. Abraham, "Preprocessing for High Resolution Beamforming," Proc. of 23rd Asilomar Conf. on Signals, Systems and Computers 1989 or NUSC Reprint Rpt. 8651, 3 November 1989.

[9] Burgess, K.A. and B.D. VanVeen, "Improved Adaptive Detection Performance via Subspace Processing," Proc. ICASSP 1992, pp.V-353-356.

[10] Hodgkiss, W.S. and L.W. Nolte, "Covariance between Fourier coefficients representing the time waveforms observed from an array of sensors," Journal of Acoustical Society of America, Vol. 59, No. 3, pp.582-590, March 1976.

[11] Goodman, N.R., "Statistical Analysis Based on a Certain Multivariate Complex Gaussian Distribution (An Introduction)," The Annals of Mathematical Statistics, Vol. 34, pp.152-177, March 1963.

[12] Baggenstoss, P.M. and S.M. Kay, "An Adaptive Detector for Deterministic Signals in Noise of Unknown Spectra Using the Rao Test," IEEE Trans. on Signal Processing, Vol. 40, No. 6, pp1460-1468, June 1992.

[13] Whalen, A.D. *Detection of Signals in Noise*, Academic Press, Inc., 1971.

[14] Owsley, N.L., "A Standardized Test Case (STC) for Sensor Array Processor Evaluation," IEEE Oceans '91 Conf. Proc. or NUSC Reprint Rpt. 8981, 20 November 1991.

[15] Muirhead, R.J., *Aspects of Multivariate Statistical Theory*, John Wiley & Sons, 1982.

[16] Press, W.H., B.P. Flannery, S.A. Teukolsky, W.T. Vetterling, *Numerical Recipes in Fortran Second Edition*, Cambridge University Press, 1988.

NUWC Technical Memorandum No. 941021

DISTRIBUTION LIST, EXTERNAL

T. G. Goldsberry	ONR 451
L. Jacobi	ONR451
N. Harned	ONR 451
J. Polcari	PEO USW ASTO
R. Holland	SPAWAR
R. Young	Penn State
J. Wolcin	USCGA
I. Metal	Norden Systems

NEW LONDON

D. Abraham (5)	2121
G. C. Carter	2192
W. Chang	3314
G. Connolly	2192
R. Dwyer	3331
J. Fay	3331
M. Gouzie	2121
S. Greineder	2121
R. Kneipfer	214
P. Koenigs	3112
J. Ianniello	2123
R. Latourette	2152
D. Lerro	3314
T. Luginbuhl	2121
A. Nuttall	302
J. Nuttall	2121
N. Owsley	2123
J. Sanchis	2152
M. Schindler	2121
D. Sheldon	3314
E. Siborg	2111
Library	(4)

NEWPORT

R. Streit	22101
Library	(2)

WEST PALM

R. Kennedy	3802

Total (40)